POLITECNICO DI TORINO

Masters of Science
in Mechanical Enginneering

Master Thesis

A Bi-fidelity strategy for the Finite Element Analysis of an electric kick scooter

Supervisor
Prof. Claudio Canuto

Candidate
Tintu Mathew

Signature of the Supervisor

. . . . . .

Signature of the Candidate

. . . . . .

Academic Year 2021-2022

† *To Appa and Amma*
† *To Greta Jurgaitytė*

Summary

This study deals with simulation Finite Element Analysis (FEA) model of the electric scooter frame under variable load conditions done both with first order elements and second order elements and the comparison and optimization using Numerical modelling.The objective of the thesis is the design, analysis and optimization of frame of the electric scooter, computing the structural analysis of the system using Altair Hypermesh®, Optistruct®, considering both first order and second order elements and verifying them using Matlab. A maximum passenger weight of 100kg is used to determine the deformations on the frame. A study of variable loads with different numbers of loads in about 20 locations in the frame has been done. The frame was considered as a static frame with a single point load acting on it. FEA simulation has been on a model based on recycled plastic. Resultant displacement vector values of the frame elements were obtained performing simulations in Altair Hypermesh. The results were then verified using Matlab to perform numerical calculations to verify the impact of high-fidelity elements over low-fidelity theory.

Acknowledgements

Foremost, I would like to express my sincere gratitude to my supervisor Prof. Claudio Canuto whose expertise was invaluable in formulating the thesis and methodology. His immense knowledge, enthusiasm, patience and scholarly advice helped me in all the time of research and writing of this thesis. I could not have imagined having a better advisor and mentor.

Besides my advisor, I would like to thank Mr. Vincenzo Stirparo, CEO, Kite Group Srl for giving me the privilege to undertake this research with Ikaros Mobility®. He has been a huge inspiration for me.

I would like to thank my parents, Shaji Mathew and Leena Mathew for all the support that they have given me not only in completing this thesis, but the love and motivation that I received during the difficult times in my academic career. Without them, I know that none of this would have been possible, and I am eternally grateful.

A special mention goes to my friends Nikhil, Suneeth, Nidhin, Merve, Guilia, Greta, Anagha and Elina for all their unconditional love and support throughout these tough times and for never giving up on me.

Contents

List of Tables

List of Figures

Part I

FEA of a scooter

Chapter 1

Introduction

1.1 General Principles

Transportation sector is undergoing a huge transformation, now more than ever the importance of sustainable solutions for an environmentally friendly future has arisen. Electric Vehicles are a perfect answer to the problem but just electrification alone will not solve the issue, as engineers we need to think beyond engines and batteries. We need to think about how production and development can help sustainability. Electric mobility will play a key role for a sustainable future transportation. As a further solution, Micro-Mobility or last mile transportation came in-to play with an idea of using electric bikes, electric kick scooters etc.

The use of micro-mobility can help boost the use of electric transportation by providing last mile solutions like covering short distances from metro stations to home or offices or from bus stops to home or offices or covering short distances for shopping or moving around in cities. Benchmarks were done with various top scooters in the market to produce top notch Electric scooter.

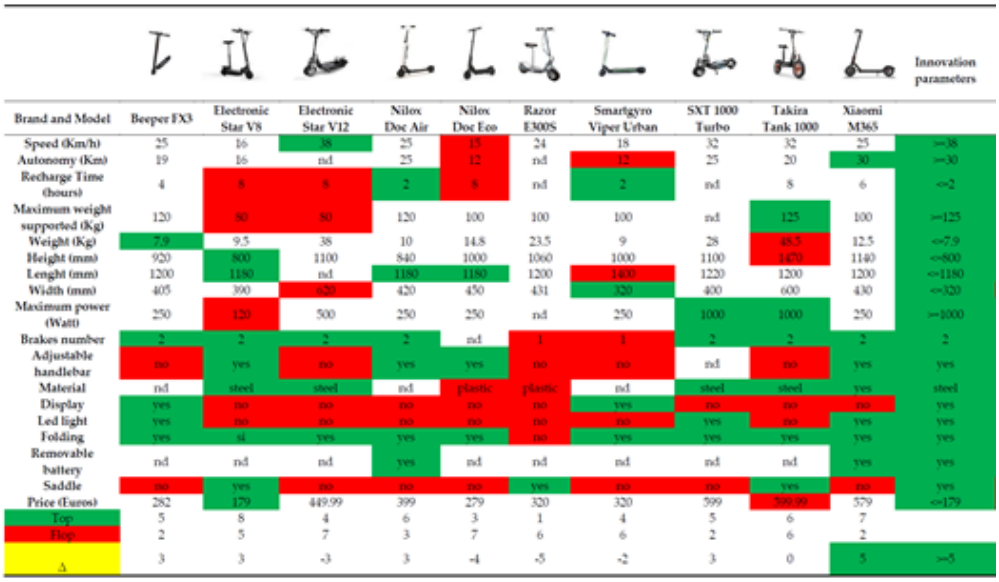

Brand and Model	Beeper FX3	Electronic Star V8	Electronic Star V12	Nilox Doc Air	Nilox Doc Eco	Razor E300S	Smartgyro Viper Urban	SXT 1000 Turbo	Takira Tank 1000	Xiaomi M365	Innovation parameters
Speed (Km/h)	25	16	38	25	15	24	18	32	32	25	>=38
Autonomy (Km)	19	16	nd	25	12	nd	12	25	20	30	>=30
Recharge Time (hours)	4	8	8	2	8	nd	2	nd	8	6	<=2
Maximum weight supported (Kg)	120	80	80	120	100	100	100	nd	125	100	>=125
Weight (Kg)	7.9	9.5	38	10	14.8	23.5	9	28	48.5	12.5	<=7.9
Height (mm)	920	800	1100	840	1000	1060	1000	1100	1470	1140	<=800
Lenght (mm)	1200	1150	nd	1180	1180	1200	1400	1220	1200	1200	<=1180
Width (mm)	405	390	620	420	450	431	320	400	600	430	<=320
Maximum power (Watt)	250	120	500	250	250	nd	250	1000	1000	250	>=1000
Brakes number	2	2	2	2	nd	1	1	2	2	2	2
Adjustable handlebar	no	yes	no	yes	yes	no	no	nd	no	yes	yes
Material	nd	steel	steel	nd	plastic	plastic	nd	steel	steel	yes	steel
Display	yes	no	no	no	no	no	yes	no	no	no	yes
Led light	yes	no	no	no	no	no	no	yes	no	yes	yes
Folding	yes	si	yes	yes	yes	no	yes	yes	yes	yes	yes
Removable battery	nd	nd	nd	yes	nd	nd	nd	nd	nd	yes	yes
Saddle	no	yes	no	no	no	yes	no	no	yes	no	yes
Price (Euros)	282	179	449.99	399	279	320	320	599	599.99	379	<=179
Top	5	8	4	6	3	1	4	5	6	7	
Flop	2	5	7	3	7	6	6	2	6	2	
Δ	3	3	-3	3	-4	-5	-2	3	0	5	>=5

Figure 1.1. Bench Marking Analysis of electric scooters in the market.

Frizziero et al. [2018]

Ikaros Mobility® came up with a perfect solution to answer all the last mile problems. Built with a completely green energy following the European regulations with "PEDELEC" (push assist) technology and the frame engineered using recycled materials. The idea around the frame was it should be lightweight but durable and strong at the same time. A research was conducted using various criteria like weight, range, features etc., meaning that qualitative and quantitative data was used as the basis for this study. The theoretical and the research analysis was based on these parameters, which helped determine the technical requirements we needed to achieve. The data researched and analysed from the market helped build a unique, one of a kind electric kick-scooters. Simulation FEA is used to analyse the frame by the designer and engineer. They aim to get light weight, durable, stiff, easy to manufacture and low production cost. An Ideal frame is manufactured by increasing mechanical properties and decreasing weight. The main priority to gain the best performance of a frame is by balancing priorities for key requirements, minimizing the mass of the frame, ideal lateral stiffness, maximizing the strength capabilities of the frame to carry load and absorb road shocks, and adjusting the vertical stiffness of the frame to provide a smooth ride.

1.2 Modelling

1.2.1 CAD Design

The model was modelled using CATIA, which was designed ergonomically, aesthetically and also keeping in mind practicality. The designs are also done so that it follows the European standards (EN 14619) and do pass the various tests prescribed in it.

Figure 1.2. Generic View

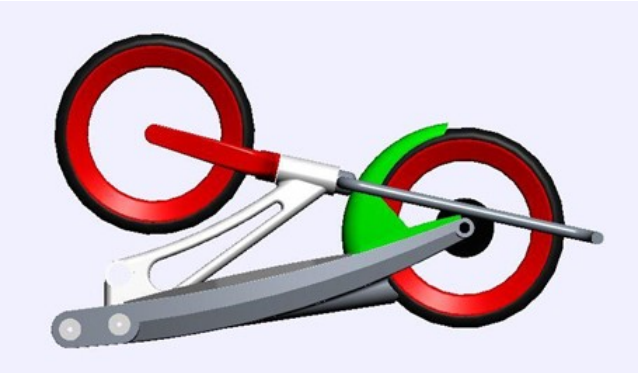

Figure 1.3. Folded View

The handlebars will be made of steel, the fork and the neck in aluminium and the frame by PBT+PET GF30. This material for the frame was chosen to keep it lightweight and durable and most importantly environmentally friendly because the material was made from recycled materials.

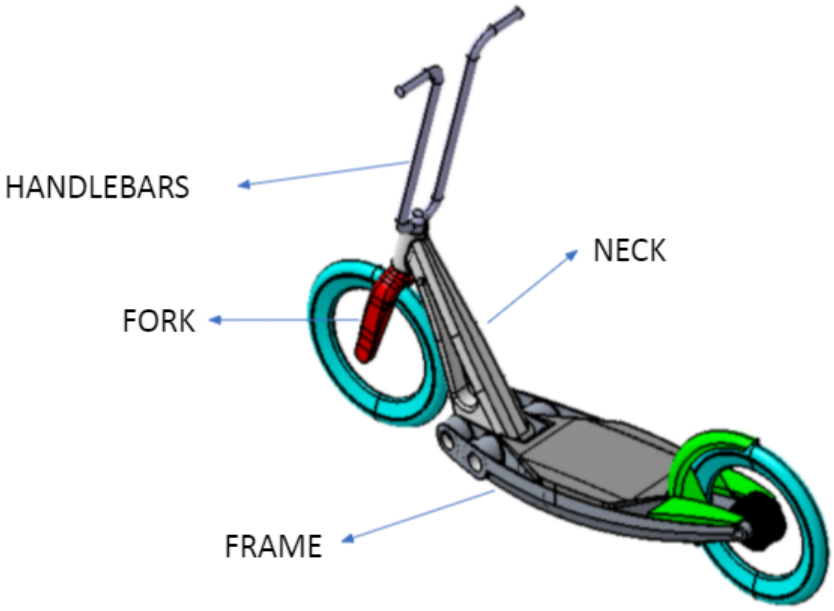

Figure 1.4. Part Description

Chapter 2

FEA Modelling

The frame model for FEA simulation is simplified by modelling in Hypermesh using tetrahedral elements to reciprocate the construction of the plastic component.

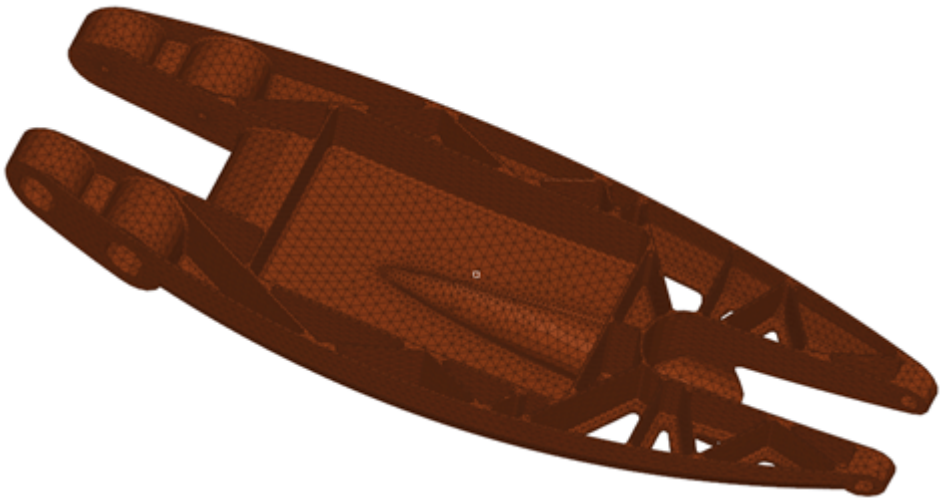

Figure 2.1. Meshed Model

A load of 1000N is applied on the centre of the frame to simulate the weight of a person on top of the scooter. The constraints are placed at the front and back, the front constraint is the connection with the neck and the rear constraint is the connection with the rear wheel.

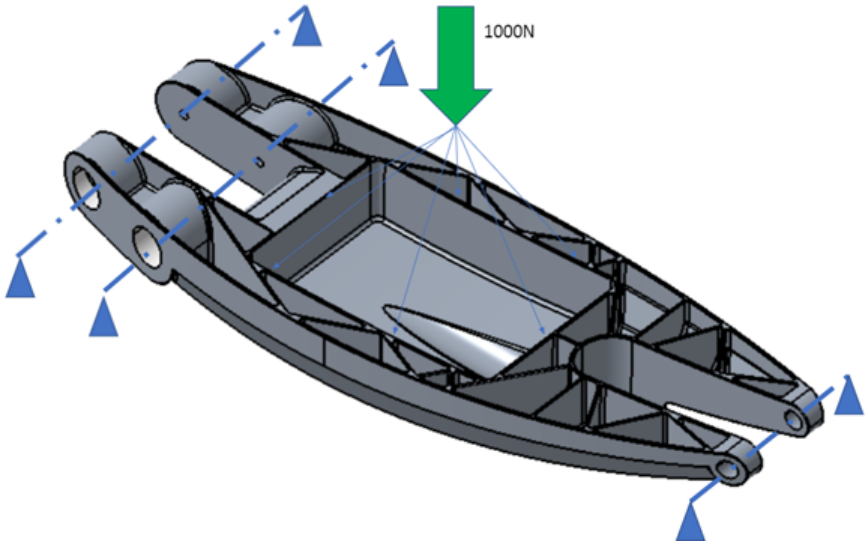

Figure 2.2. Loads and Constraints

The frame is modelled using multiple ribs to increase the part stiffness while keeping the mass low as possible.

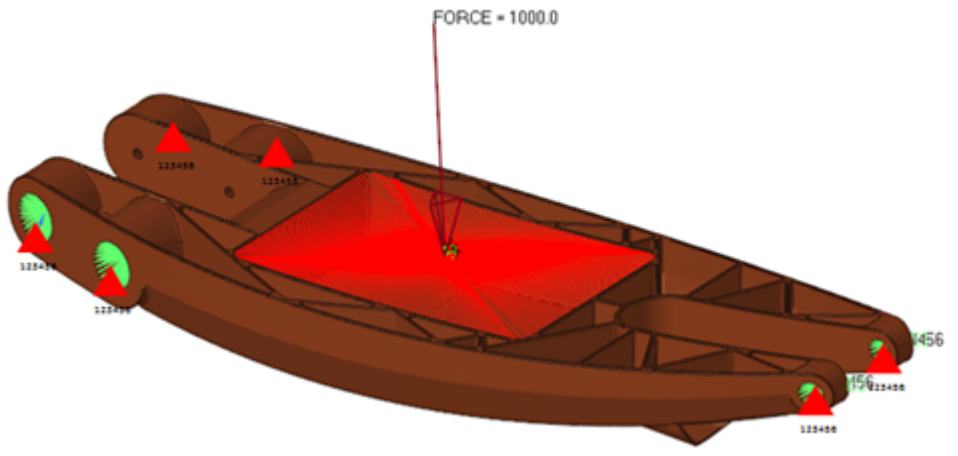

Figure 2.3. Post Processed Model

2.1 Material

The material used is Ultradur® B 4040 G6 (PBT+PET)-GF30 at 23°C From BASF which has the following material specifications:

Young's modulus: 6862 MPa Yield Strength: 99 MPa Strain Rate: 1.7 %

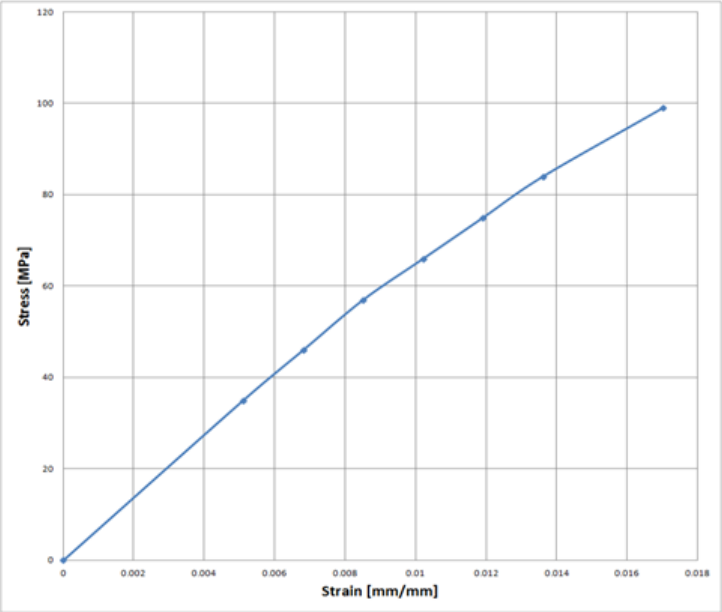

Figure 2.4. Material S-N Curve

The mesh is done in different mesh sizes., i.e. 5mm and 10mm and also in both first order and second order elements, to observe the difference in results with respect to the computing time.

2.2 Element Type

Using the image Nastran [2019] of the low-fidelity solid tetrahedral element we can see that the origin of the element coordinate system is at G1. The element x-axis is defined by the vector G1 –G2. The element y-axis is orthogonal to the element x-axis and is in the G1-G2-G3 plane.

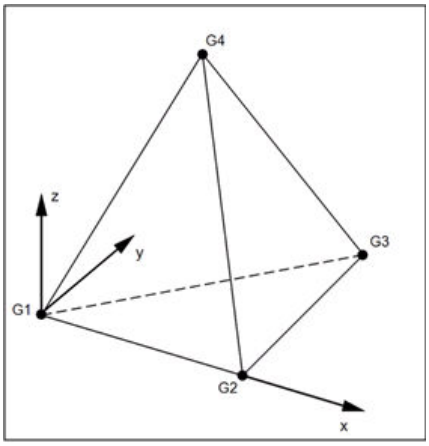

Figure 2.5. low-fidelity Element

The element z-axis is found using the cross product of element x and element y. There are two forms of solid tetrahedral elements used, low-fidelity and high-fidelity. Low-fidelity solid tetrahedral elements have only 4 nodes.

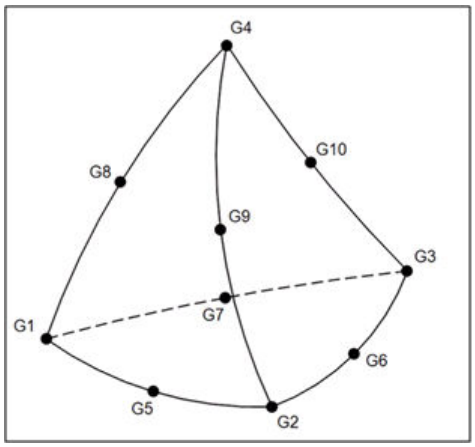

Figure 2.6. high-fidelity Element

High-fidelity solid tetrahedral elements have 10 nodes. Low-fidelity solid tetrahedral elements are stiffer while the high-fidelity elements are more flexible. Solid elements do not have rotational degrees of freedom at each node. A moment or a torque applied to the face of a solid element mesh (low or high-fidelity) will result in zero or null output. A force couple or rigid

element must be used to apply a torque or moment to a surface that has an associated solid mesh. All solid element results are given in the global rectangular coordinate system. The solid elemental results are the result of averaging the Gaussian point results. The nodal results (or corner results) are extrapolated to the node using the nearby Gauss point and the shape functions of the elements.

The first-order triangle and tetrahedron are constant stress elements and use a single integration point for the stiffness calculation when used in stress/displacement applications. A lumped mass matrix is used for both elements, with the total mass divided equally over the nodes. For heat transfer applications a three-point integration scheme is used for the conductivity and heat capacity matrices of the first-order triangle, with the integration points midway between the vertices and the centroid of the element; and a four-point integration scheme is used for the first-order tetrahedron. Distributed loads are integrated with two and three points for first-order triangles and tetrahedrons, respectively.

The three-point scheme is also used for the stiffness of the second-order triangle when it is used in stress/displacement applications. The mass matrix is integrated with a six-point scheme that integrates fourth-order polynomials exactly Cowper [1973]. Distributed loads are integrated using three points. The heat transfer versions of the element use the six-point scheme for the conductivity and heat capacity matrices.

For stress/displacement applications the second-order tetrahedron uses 4 integration points for its stiffness matrix and 15 integration points for its consistent mass matrix. For heat transfer applications the conductivity and heat capacity matrices are integrated using 15 integration points. The first-order wedge uses 2 integration points for its stiffness matrix but 6 integration points for its lumped mass matrix. The second-order wedge uses 9 integration points for its stiffness matrix but 18 integration points for its consistent mass matrix. Stroud [1971]

2.3 Simulation Results

5mm Low-fidelity Tetra Mesh

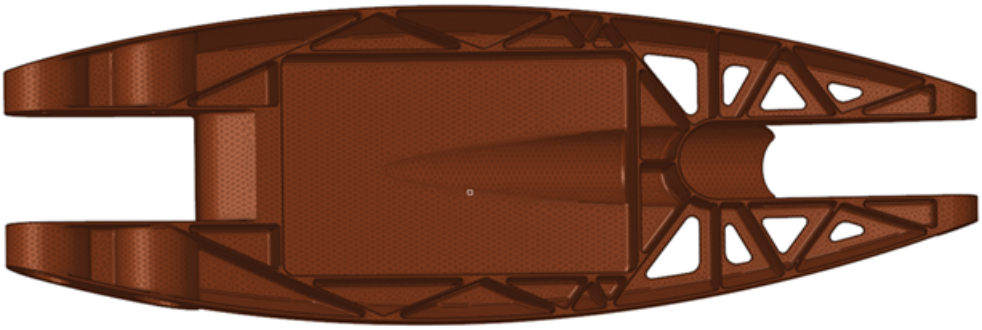

Figure 2.7. Meshed Component

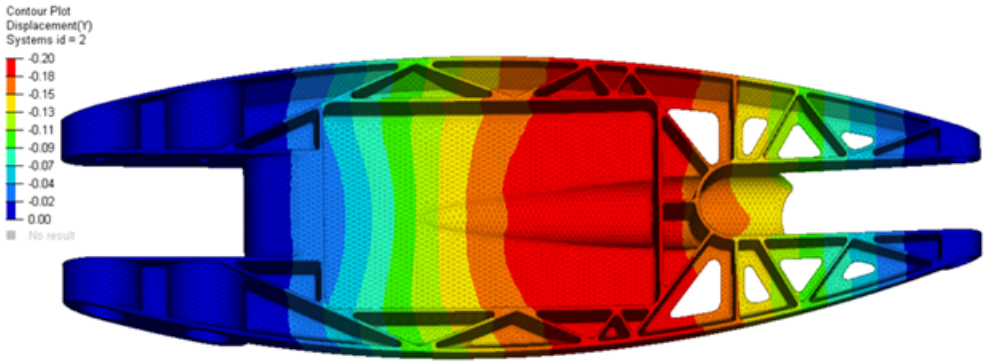

Figure 2.8. 5mm 1st Order- Displacement Results

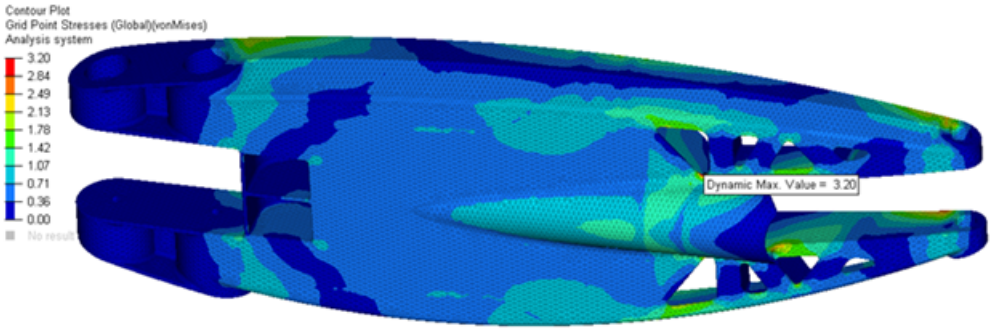

Figure 2.9. 5mm 1st Order - Von Mises Stress Results

5mm High-fidelity Tetra Mesh

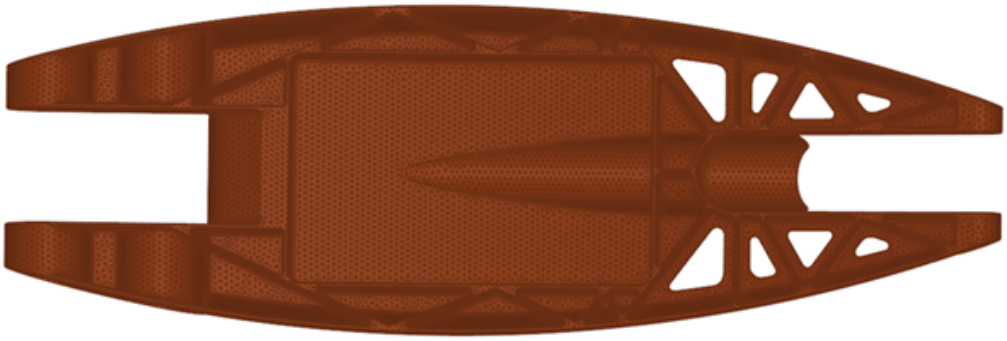

Figure 2.10. Meshed Component

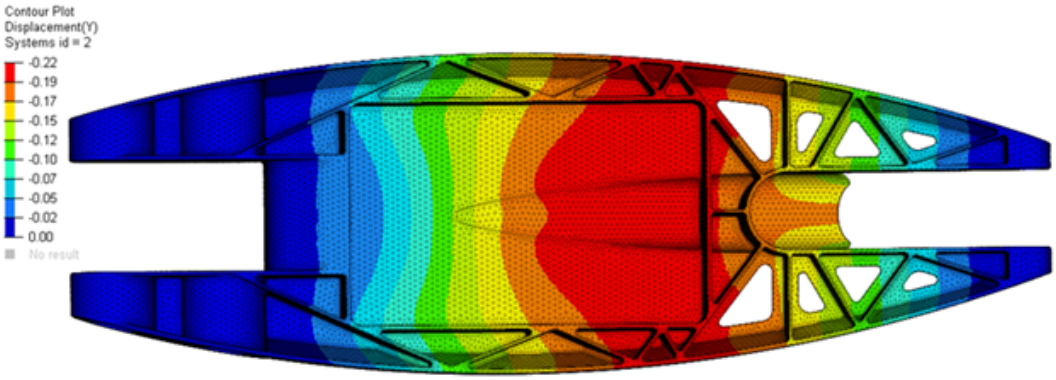

Figure 2.11. 5mm 2nd Order- Displacement Results

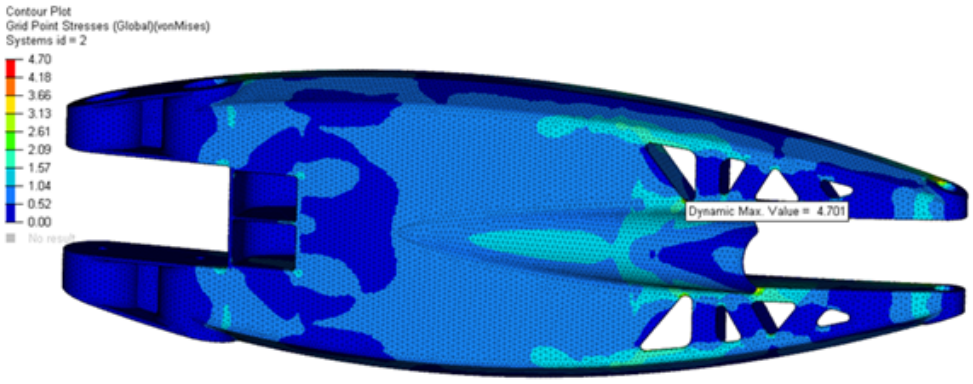

Figure 2.12. 5mm 2nd Order - Von Mises Stress Results

10mm Low-fidelity Tetra Mesh

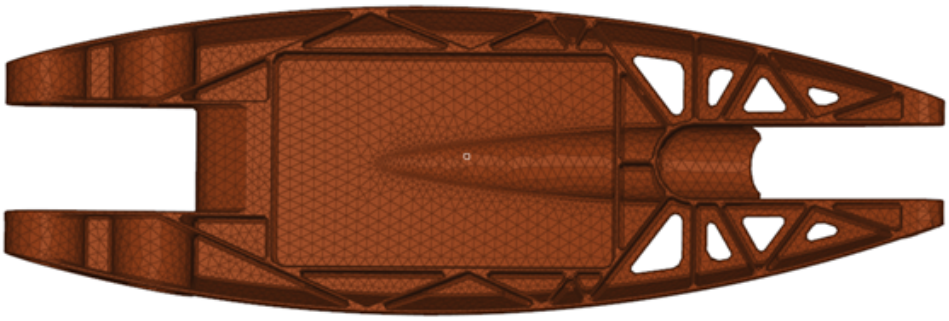

Figure 2.13. Meshed Component

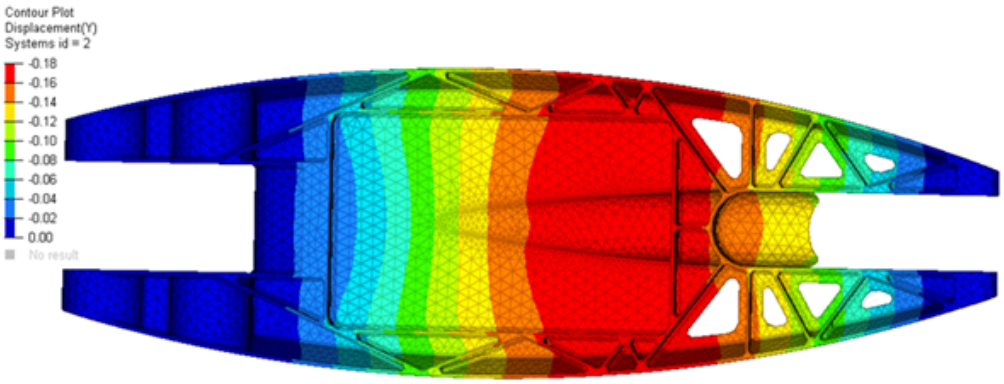

Figure 2.14. 10mm 1st Order- Displacement Results

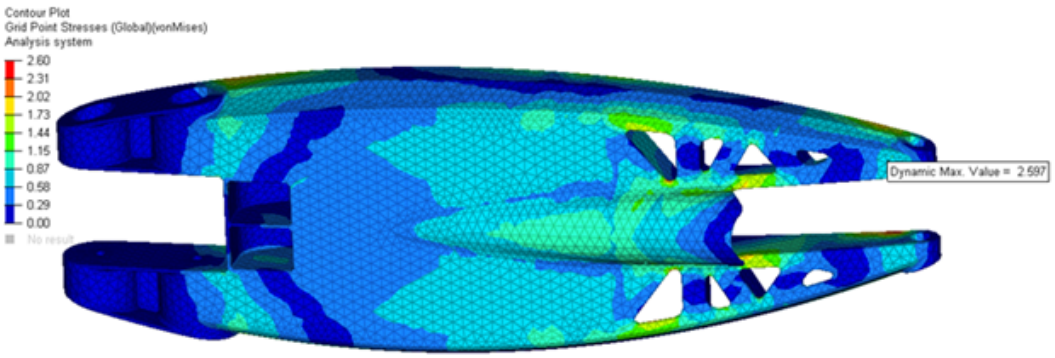

Figure 2.15. 10mm 1st Order - Von Mises Stress Results

10mm High-fidelity Tetra Mesh

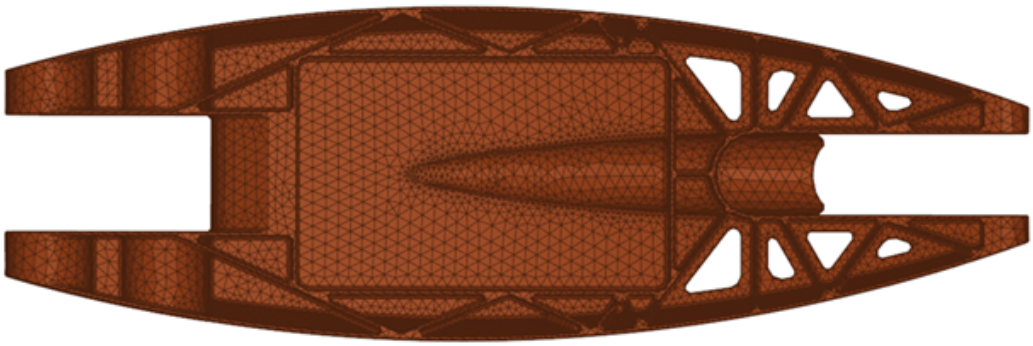

Figure 2.16. Meshed Component

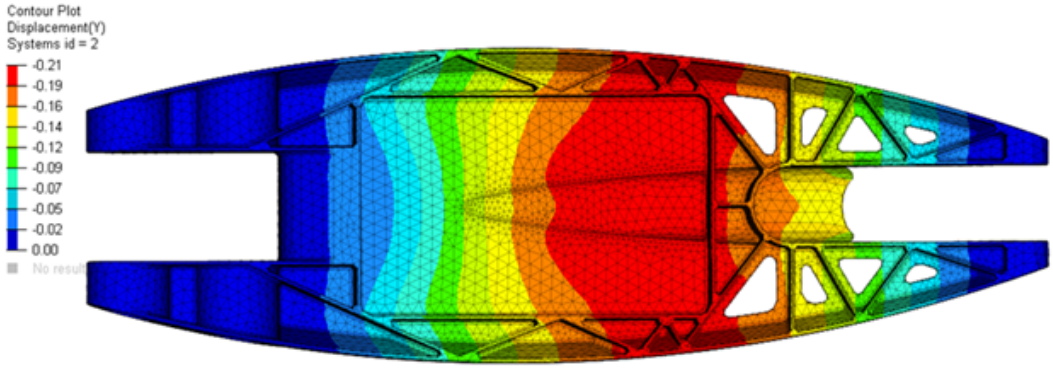

Figure 2.17. 10mm 2nd Order- Displacement Results

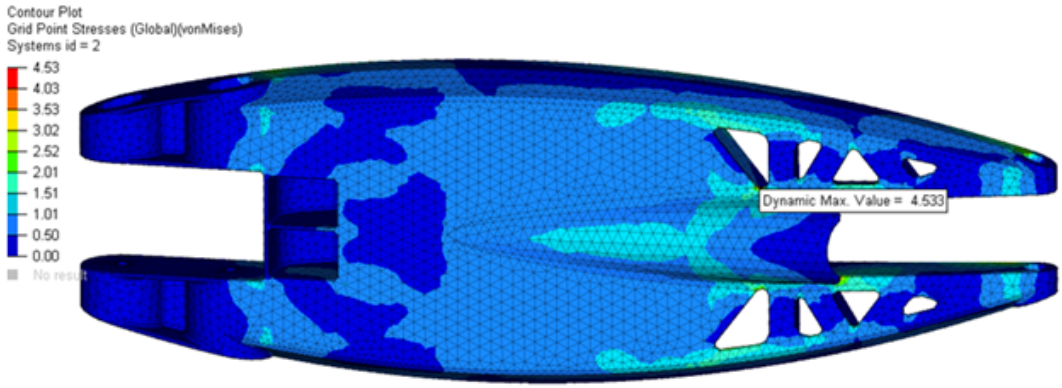

Figure 2.18. 10mm 2nd Order - Von Mises Stress Results

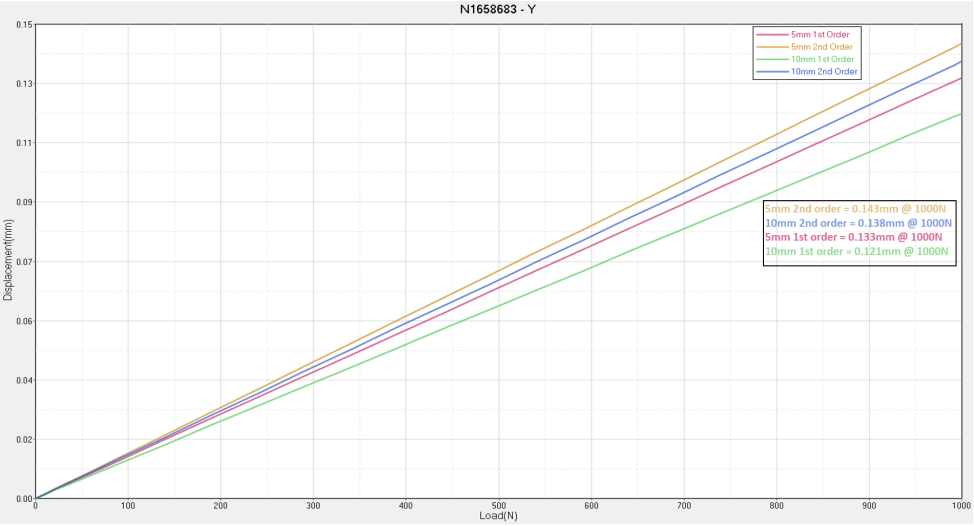

Figure 2.19. Load vs Displacement

	Number of Node	Computing Time (mins)	Displacement (mm)	Von Mises Stress (Mpa)
5mm 1st order	64954	11	0.133	3.20
10mm 1st order	17405	6	0.121	2.59
5mm 2nd order	405079	59	0.143	4.70
10mm 2nd order	106246	23	0.138	4.5

Table 2.1. Values of various mesh sizes

From the above data we can see that the 2nd order 5mm elements give the most accurate results but the computation time is almost double of the other elements which is a disadvantage in terms of time. This bring us to developing a solution of where we can extrapolate the results of the 2nd order elements using the results of the 1st order elements, so that we can save a lot of time and get the same results as 2nd order.

Part II

Bi-fidelity Analysis

Chapter 3

The Bi-fidelity Algorithm

3.1 General Principles

A bifidelity strategy Canuto et al. [2019] is applied to the computation of mechanical piece of interest which depends in a arbitrary pattern. The procedure applies the precision of a high-fidelity model and the efficiency of a low-fidelity model, obtained through the use of different iterations of numerical solutions, to pursue a high quality approximation of the statistics with a moderate number of high-fidelity simulations. In both applications, the results highlight the efficacy of the approach in terms of error decay versus the number of computed high-fidelity solutions, even when the QoI lacks smoothness. The observed gain in computational cost is at least of one order of magnitude.
The combined use of multiple computational models to simulate a physical situation of interest has become a common practice in applied Science and Engineering, and it is gaining increasing popularity among practitioners. Typically, one creates a model which presents them with precise accuracy in the simulation but at an expensive computational cost, this will be referred to as the 'high-fidelity' model. When one or more models are available, that presents lower levels of accuracy but at low computational costs; these will be the 'low-fidelity' models. For example, one can go from high-to low-fidelity models by reducing the complexity in the mathematical model of interest; another common option is to the use the same mathematical model, but reducing the number of nodes and mesh quality to create a coarse mesh. Bi-fidelity methods aim at obtaining a high-fidelity accuracy with low-fidelity computational times, in such a way that the resulting accuracy is comparable

to that of the high-fidelity model but the resulting cost is comparable to that of the low-fidelity model. This is possible when the response of the model exhibits a low-rank dependence upon the input data, that can already be captured sufficiently well through the information provided by the low-fidelity models. We have done various high-fidelity simulations and the equal number of low-fidelity simulations and obtained the results of the both the set of simulations to input them into MATLAB code.

3.2 Methodology

A configuration of mechanical piece of interest depends upon d parameters $z_1, z_2, ...z_d$ and can be described by c variables as $u_1, u_2, ...u_c$. We write that $\underline{z} = (z_1, z_2, ...z_d) \in \mathcal{Z} \subset \mathcal{R}^d$ for the set of admissible parameters and $\underline{u} = (u_1, u_2, ...u_d)^T \in \mathcal{R}^c$ for the set of resulting configurations we write

$$\underline{u} = \underline{u}(\underline{z})$$

to indicate that the configuration of $\underline{u}$ is obtained from the parameters of $\underline{z}$. In practice, the computation of the output $\underline{u}$ is gotten from the input $\underline{z}$ which is performed by a FEM simulation, so its only approximate. In practice, we use two codes, one is low-fidelity which cheaper but with low accuracy while the other is high-fidelity which is expensive but the accuracy is high. Let us denote by

$$\underline{u}^L(\underline{z}) \ , \underline{u}^H(\underline{z}) \text{ respectively.},$$

the approximate configurations obtained by the low-fidelity simulation by the high-fidelity code respectively.
We chose a finite subset $\Gamma \in \mathcal{Z}$ in the parameter space, which contains M vectors of parameters, which will be sufficiently significant to describe the parameter space. For each $\underline{z} \in \Gamma$, we compute the corresponding configuration $u^L(z)$ by the low-fidelity simulation, assuming $U^L(\Gamma) = \{\underline{u}^L(\underline{z}) : \ \mathcal{Z} \subset \Gamma\}$ will be the set of these configurations. We also would like to compute the high-fidelity configurations for $\mathcal{Z} \subset \Gamma$ i.e., $U^H(\Gamma) = \{\underline{u}^H(\underline{z}) : \ \mathcal{Z} \subset \Gamma\}$ but this will be quite expensive to compute. So we have to try a different approach to compute the approximations $\tilde{\underline{u}}^H(\underline{z}) \ of \ \underline{u}^H(\underline{z})$ but computing only few variables of $|\underline{u}|^H(\underline{z})$, we take $N << M$ of them, and for the remaining $|\underline{z}|$ we will use the information obtained by the $\underline{u}^L(\underline{z})$.

We have ordered the set Γ of parameter vectors as

$$\underline{z}_1 \ , \underline{z}_2 \ , \underline{z}_3 \ , ..., \underline{z}_M \text{ in general } \underline{z}_m \quad 1 \leq m \leq M$$

we have taken each $\underline{z}_m$ is a vector in $\mathcal{R}^d$, which is convenient to think as a row vector

$$z_{[m]} = (z_{[m]_1} \ , \ z_{[m]_2} \ , ..., z_{[m]_d}) \in \mathcal{R}^d.$$

We denote by

$$\underline{\mathrm{U}}^L \ = \underline{\mathrm{U}}^L \ (\Gamma)$$

the set of low order configurations corresponding to the parameters in Γ. Each $\underline{\mathrm{u}}^L_{[m]} \ = \ \underline{\mathrm{U}}^L \ (z_{[m]})$ in $\underline{\mathrm{u}}^L_\Gamma$ is a vector in $\mathcal{R}^d$ which is convenient to think as a column-vector

$$\underline{\mathrm{u}}^L_{[m]} \ = (\underline{\mathrm{u}}^L_{[m]_1} \ , \underline{\mathrm{u}}^L_{[m]_2} \ , ..., \underline{\mathrm{u}}^L_{[m]_d})^T = \begin{bmatrix} u^L_{[m]_1} \\ u^L_{[m]_2} \\ . \\ . \\ u^L_{[m]_d} \end{bmatrix} \in \mathcal{R}^d \tag{3.1}$$

We form the matrix $V \in \mathcal{R}^{(\ p \times \ M\ )}$ (p rows, M columns) containing the vectors $\underline{\mathrm{u}}^L_{[m]_1}$

$$V = \begin{bmatrix} & & & & \\ \underline{\mathrm{u}}^L_{[1]} & \underline{\mathrm{u}}^L_{[2]} & . & . & \underline{\mathrm{u}}^L_{[m]} \\ & & & & \end{bmatrix} \tag{3.2}$$

Then, we form the Gramian matrix G of $V^TV \in R^{(M\times M)}$ and perform its Choleski decomposition HH^T. Next we apply a column-pivoted QR decomposition of the matrix VH to get

$$VH = QRP^T \tag{3.3}$$

Where P is the permutation matrix.
The matrix P corresponds to the reordering of the indices of m, namely

$$m_1, m_2, m_3.....$$

according to the importance.
Correspondingly we obtain a reordering of vectors in $\underline{\mathrm{u}}^L(\Gamma)$ namely

$$\underline{\mathrm{u}}^L_{[m_1]}, \underline{\mathrm{u}}^L_{[m_2]}, \underline{\mathrm{u}}^L_{[m_3]}.....$$

We then pick the first $N << M$ vectors in this ordered list, this way we have selected a subset $\gamma_N \subset \Gamma$ of parameter vectors i.e.,

$$\gamma_N = \left\{\underline{\mathrm{z}}_{[m_1]}, \underline{\mathrm{z}}_{[m_2]}, ..., \underline{\mathrm{z}}_{[m_N]}\right\} \tag{3.4}$$

and correspondingly a subset of

$$U^L(\gamma_N) = \left\{\underline{\mathrm{z}}_{[m_1]}, \underline{\mathrm{z}}_{[m_2]}, ..., \underline{\mathrm{z}}_{[m_N]}\right\}. \tag{3.5}$$

From the assumption that N is significantly smaller than M, we can afford to compute the high-fidelity approximations

$$\underline{u}^H_{[m_1]}, \underline{u}^H_{[m_2]}, ..., \underline{u}^H_{[m_N]}$$

from which we get the subset of

$$U^L(\gamma_N) \tag{3.6}$$

For any $\underline{z} \in \Gamma$, we have defined the approximation $\underline{\tilde{u}}^H(\underline{z})$ of $\underline{u}^H(\underline{z})$ by the following formula

$$\underline{\tilde{u}}^H(z) = \sum_{k=1}^{N} c_k \underline{u}^H_{[m_k]} \tag{3.7}$$

where the coefficient c_k are given by the solution of the linear system

$$\tilde{G}c = g$$

,

in which $\tilde{G}$ is the truncated Gramian matrix and the elements of g are given by

$$g_k = (\underline{u}^L(\underline{z}))^T(\underline{u}^L_{[m_k]})$$

With these values in hand we can monitor the approximation error.

$$||\underline{\tilde{u}}^H(z) - \underline{u}^H_{(z)}|| \tag{3.8}$$

Part III

Applications

Chapter 4

Matlab Simulations

4.1 First test case

The first test was performed with 20 different simulations in Altair Hypermesh® with application of a load of 1000N directly to the element, which will be uniformly distributed to the elements. The post-processing was done using Optistruct® to produce the displacement vectors in X,Y and Z directions which is used to do the analysis in MATLAB.

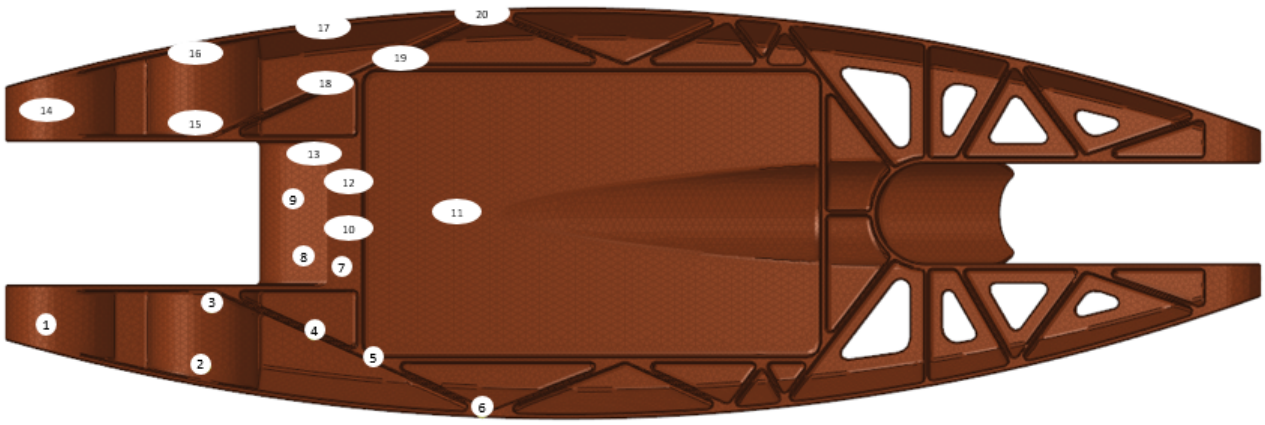

Figure 4.1. Loading Points

The displacement vectors were created from the X,Y and Z components of the 13 different nodes, the same 13 nodes were used for the 20 simulations.

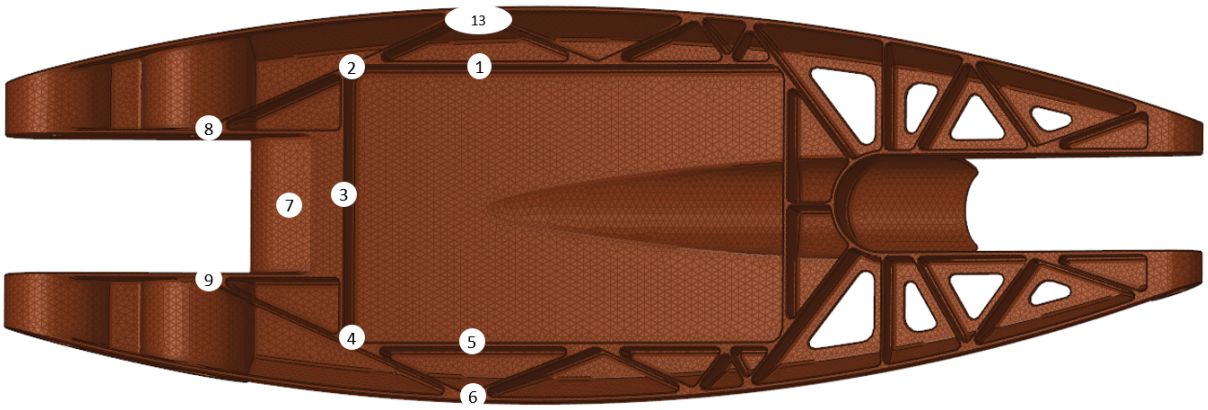

Figure 4.2. Displacement Points

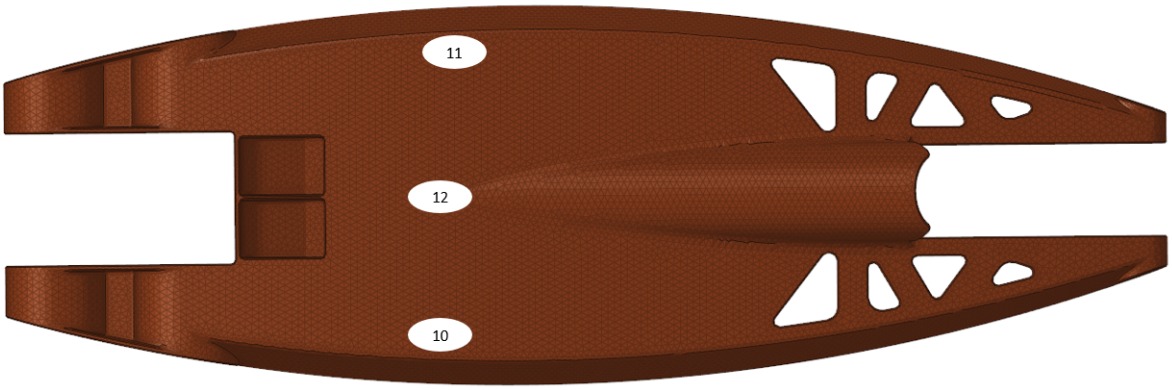

Figure 4.3. Displacement Points

This approach had its flaws, the results were inaccurate and not reliable. This was observed to be due to the wide scattering of the displacement noted from which the vectors were obtained.

4.2 Second test case

The second test was done with 30 different simulations in Altair Hypermesh® with applying a load of 1000N directly to the element, which will be uniformly distributed to the elements. The displacement vectors were created from the X,Y and Z components of from 12 different nodes of the 30 simulations, which was chosen in the same zone, the number of simulations were increased to get more data.

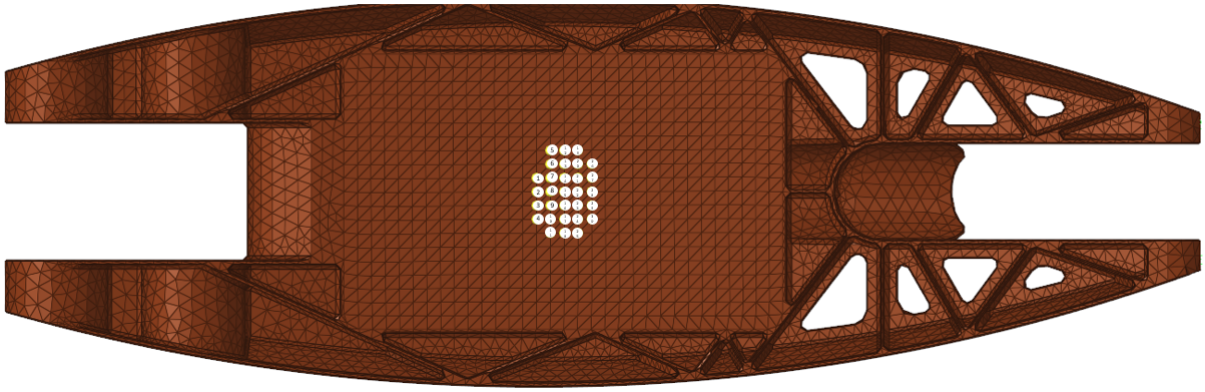

Figure 4.4. Loading Points

The displacement nodes were selected from a zone close to the loading area and in a pattern close to each other.

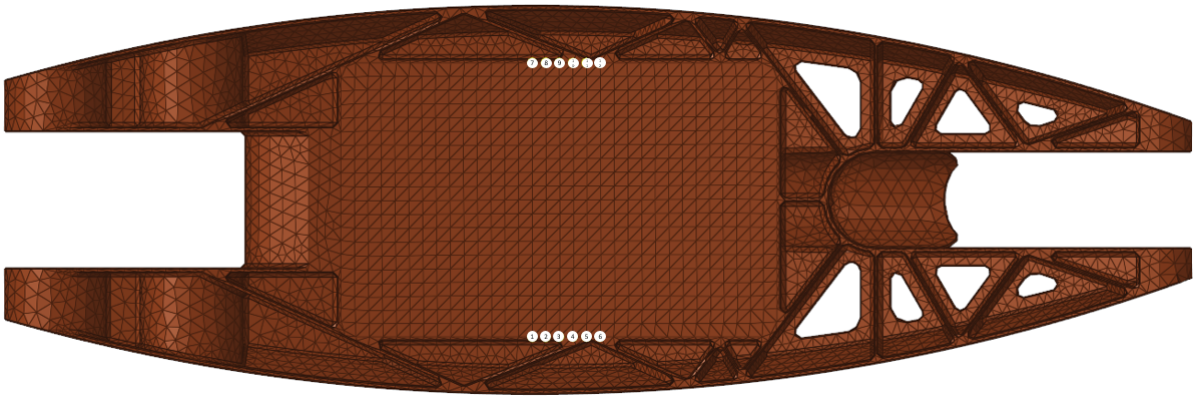

Figure 4.5. Displacement Points

The 30 displacement vectors computed with the high-fidelity vectors are reported in the Appendix A.1, and those computed with the low-fidelity vectors in the Appendix A.2. This approach gave more accurate and reliable results. The placement of loading areas and displacement vectors helped improve the analysis.

4.3 Mathematical Experiments

4.3.1 First Experiment

In this case we the high-fidelity vectors same as the low-fidelity vectors.

Reconstructed Vectors	5 Vectors	10 Vectors	15 Vectors	20 Vectors
1	0.0E+00	0.0E+00	0.0E+00	0.0E+00
2	0.0E+00	0.0E+00	0.0E+00	0.0E+00
3	0.0E+00	0.0E+00	0.0E+00	0.0E+00
4	0.0E+00	0.0E+00	0.0E+00	0.0E+00
5	0.0E+00	0.0E+00	0.0E+00	0.0E+00
6	2.4E-03	0.0E+00	0.0E+00	0.0E+00
7	3.2E-01	0.0E+00	0.0E+00	0.0E+00
8	2.5E-02	0.0E+00	0.0E+00	0.0E+00
9	2.6E-01	0.0E+00	0.0E+00	0.0E+00
10	1.8E-01	0.0E+00	0.0E+00	0.0E+00
11	3.8E-03	1.4E-03	0.0E+00	0.0E+00
12	2.6E-03	0.8E-03	0.0E+00	0.0E+00
13	2.4E-03	2.3E-03	0.0E+00	0.0E+00
14	4.8E-03	2.0E-03	0.0E+00	0.0E+00
15	3.7E-03	1.5E-03	0.0E+00	0.0E+00
16	3.0E-03	1.0E-03	0.9E-03	0.0E+00
17	2.6E-03	2.8E-03	0.9E-03	0.0E+00
18	2.2E-03	1.3E-03	0.7E-03	0.0E+00
19	3.6E-03	1.6E-03	0.4E-03	0.0E+00
20	4.2E-03	2.9E-03	0.5E-03	0.0E+00
21	5.0E-03	2.8E-03	0.5E-03	0.5E-03
22	3.9E-03	2.8E-03	0.7E-03	0.6E-03
23	3.6E-03	2.5E-03	0.7E-03	0.3E-03
24	3.5E-03	2.3E-03	0.8E-03	0.5E-03
25	2.6E-03	1.2E-03	1.2E-03	0.6E-03
26	3-5E-03	2.6E-03	0.8E-03	0.8E-03
27	3.6E-03	3.1E-03	0.5E-03	0.4E-03
28	3.0E-03	3.4E-03	1.0E-03	0.8E-03
29	3.6E-03	2.5E-03	0.5E-03	0.3E-03
30	1.8E-03	0.0E+00	0.0E+00	0.0E+00

Table 4.1. First Experiment

4.3.2 Second Experiment

In this case we use false high-fidelity vectors which is defined as a perturbation of the low-fidelity vectors, where the perturbed vectors are created using a random function of Matlab with keeping the epsilon value as $\epsilon = 1.e + 5$.

Reconstructed Vectors	5 Vectors	10 Vectors	15 Vectors	20 Vectors
1	0.0E+00	0.0E+00	0.0E+00	0.0E+00
2	0.0E+00	0.0E+00	0.0E+00	0.0E+00
3	0.0E+00	0.0E+00	0.0E+00	0.0E+00
4	0.0E+00	0.0E+00	0.0E+00	0.0E+00
5	0.0E+00	0.0E+00	0.0E+00	0.0E+00
6	3.8E-01	0.0E+00	0.0E+00	0.0E+00
7	4.3E-01	0.0E+00	0.0E+00	0.0E+00
8	9.2E-02	0.0E+00	0.0E+00	0.0E+00
9	1.7E-01	0.0E+00	0.0E+00	0.0E+00
10	3.1E-01	0.0E+00	0.0E+00	0.0E+00
11	1.9E-01	1.6E-01	0.0E+00	0.0E+00
12	2.4E-01	4.8E-02	0.0E+00	0.0E+00
13	3.4E-01	3.4E-01	0.0E+00	0.0E+00
14	3.3E-01	6.0E-01	0.0E+00	0.0E+00
15	2.4E-01	3.1E-01	0.0E+00	0.0E+00
16	6.5E-02	3.2E-01	7.3E-01	0.0E+00
17	4.0E-01	4.3E-01	7.3E-01	0.0E+00
18	2.7E-01	2.7E-01	7.4E-01	0.0E+00
19	1.6E-01	2.5E-01	2.6E-01	0.0E+00
20	4.1E-01	3.5E-01	2.8E-01	0.0E+00
21	2.6E-01	1.2E-01	4.2E-01	2.0E-01
22	6.7E-02	3.7E-01	3.0E-01	3.2E-01
23	3.4E-02	3.7E-01	2.5E-01	4.0E-01
24	5.3E-01	1.8E-01	1.9E-01	5.0E-01
25	2.8E-01	3.7E-01	1.5E-01	4.2E-02
26	2.1E-01	2.1E-01	3.7E-01	1.6E-01
27	1.8E-01	3.6E-01	3.1E-01	1.2E-01
28	1.5E-01	8.5E-02	1.6E-01	4.3E-01
29	5.0E-01	2.5E-01	2.5E-01	1.2E-01
30	4.0E-01	2.0E-01	8.0E-01	6.8E-02

Table 4.2. Second Experiment

We vary the *epsilon* values i.e., $\epsilon = 0, 10^{-1}$,10^{-2},10^{-3}... of the second experiment to find out the variation in the values. In this case we have taken the case where we have used 15 vectors to reconstruct the new vectors.

Reconstructed Vectors	$\epsilon = 0$	$\epsilon = 10^{-1}$	$\epsilon = 10^{-2}$	$\epsilon = 10^{-3}$
16	0.6E-03	3.3E-02	1.4E-02	3.8-03
17	0.7E-03	2.6E-02	1.1E-02	2.8E-03
18	0.9E-03	4.2E-02	0.4E-02	3.3-03
19	0.8E-03	4.4E-02	0.7E-02	3.6E-03
20	1.0E-03	3.6E-02	0.6E-02	3.3E-03
21	0.9E-03	0.1E-02	0.9E-02	4.3E-03
22	1.6E-03	5.0E-02	0.3E-02	3.0E-03
23	1.4E-03	8.5E-02	0.7E-02	5.0E-03
24	0.5E-03	1.2E-02	0.6E-02	3.7E-03
25	1.2E-03	4.3E-02	1.1E-02	5.7E-03
26	1.1E-03	0.1E-02	1.1E-02	4.6E-03
27	0.6E-03	3.0E-02	0.4E-02	4.8E-03
28	0.8E-03	9.3E-02	0.6E-02	4.1E-03
29	1.7E-03	6.3E-02	1.3E-02	3.6E-03
30	1.4E-03	7.2E-02	0.1E-02	3.6E-03

Table 4.3. Second Experiment with various ϵ values

4.3.3 Third Experiment

In this case we use the real Low-fidelity vectors and the real high-fidelity vectors.

Reconstructed Vectors	5 Vectors	10 Vectors	15 Vectors	20 Vectors
1	0.0E+00	0.0E+00	0.0E+00	0.0E+00
2	0.0E+00	0.0E+00	0.0E+00	0.0E+00
3	0.0E+00	0.0E+00	0.0E+00	0.0E+00
4	0.0E+00	0.0E+00	0.0E+00	0.0E+00
5	0.0E+00	0.0E+00	0.0E+00	0.0E+00
6	2.4E-03	0.0E+00	0.0E+00	0.0E+00
7	3.2E-03	0.0E+00	0.0E+00	0.0E+00
8	2.5E-03	0.0E+00	0.0E+00	0.0E+00
9	2.6E-03	0.0E+00	0.0E+00	0.0E+00
10	1.8E-03	0.0E+00	0.0E+00	0.0E+00
11	3.8E-03	1.4E-03	0.0E+00	0.0E+00
12	2.5E-03	8.3E-04	0.0E+00	0.0E+00
13	2.4E-03	2.3E-03	0.0E+00	0.0E+00
14	4.8E-03	2.0E-03	0.0E+00	0.0E+00
15	3.7E-03	1.6E-03	0.0E+00	0.0E+00
16	3.0E-03	1.0E-03	9.4E-04	0.0E+00
17	2.6E-03	2.8E-03	9.8E-04	0.0E+00
18	2.2E-03	1.3E-03	7.2E-04	0.0E+00
19	3.6E-03	1.6E-03	4.0E-04	0.0E+00
20	4.2E-03	3.0E-03	5.9E-04	0.0E+00
21	5.0E-03	2.8E-03	5.7E-04	5.6E-04
22	3.9E-03	2.9E-03	7.6E-04	6.0E-04
23	3.6E-03	2.5E-03	7.0E-04	3.3E-04
24	3.5E-03	2.3E-03	8.2E-04	5.7E-04
25	2.6E-03	1.3E-03	1.2E-03	6.2E-04
26	3.5E-03	2.6E-03	8.1E-04	8.1E-04
27	3.6E-03	3.1E-03	5.2E-04	3.8E-04
28	2.9E-03	3.4E-03	1.0E-03	8.5E-04
29	3.5E-03	2.4E-03	5.7E-04	3.4E-04
30	1.8E-03	0.0E+00	0.0E+00	0.0E+00

Table 4.4. Third Experiment

Plot of the vectors

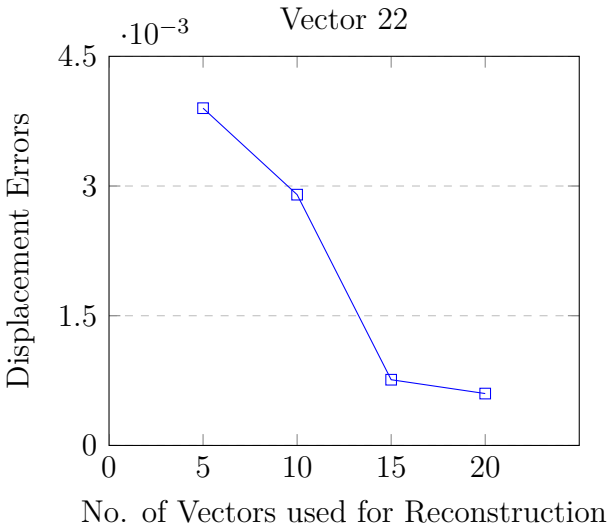

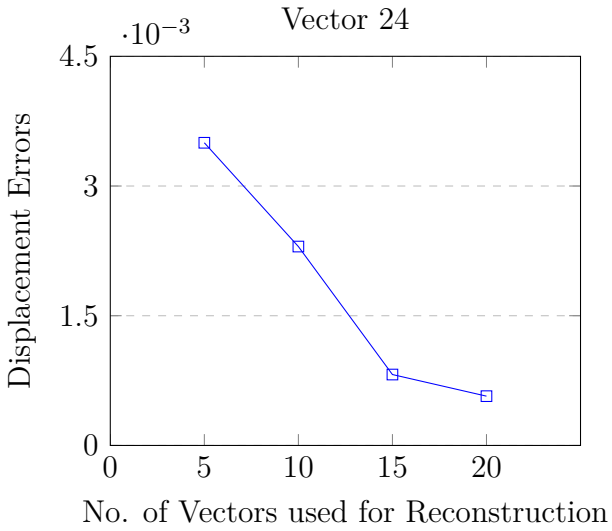

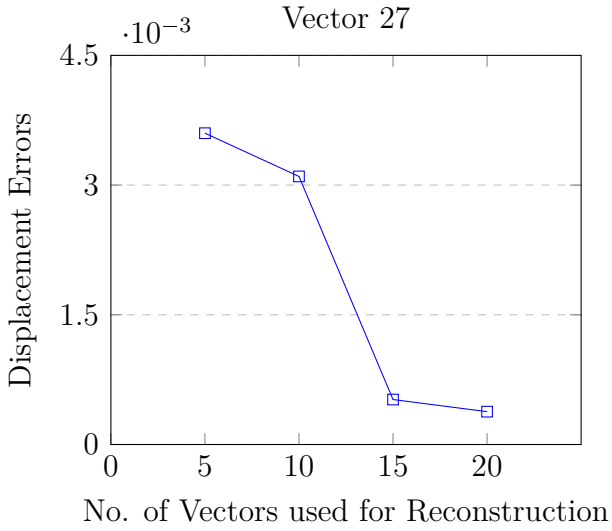

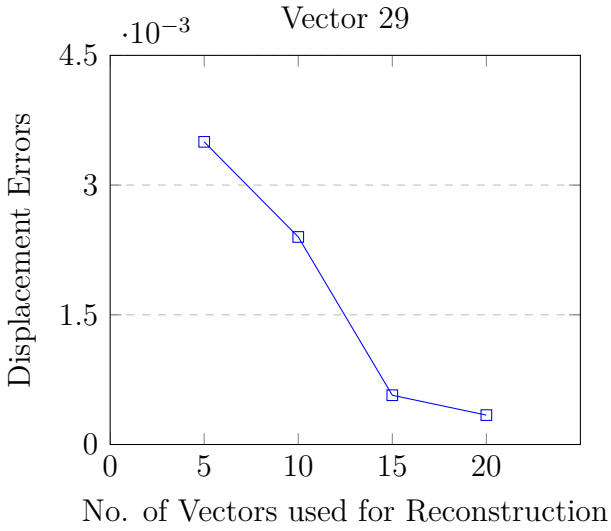

Bibliography

Claudio Canuto, Sandra Pieraccini, and Dongbin Xiu. Uncertainty quantification of discontinuous outputs via a non-intrusive bifidelity strategy. *Journal of Computational Physics*, 398:108885, 2019. ISSN 0021-9991. doi: https://doi.org/10.1016/j.jcp.2019.108885.

G. R. Cowper. Gaussian quadrature formulas for triangles. *International Journal for Numerical Methods in Engineering*, 7(3):405–408, 1973. doi: https://doi.org/10.1002/nme.1620070316.

Leonardo Frizziero, Giampiero Donnici, Daniela Francia, Alfredo Liverani, Gianni Caligiana, and Francesco Di Bucchianico. Innovative urban transportation means developed by integrating design methods. *Machines*, 6(4), 2018. ISSN 2075-1702. doi: 10.3390/machines6040060. URL https://www.mdpi.com/2075-1702/6/4/60.

Autodesk Nastran. Finite elements in autodesk nastran in-cad. 2019. URL https://help.autodesk.com/view/NINCAD/2019/ENU/.

A. H Stroud. Approximate calculation of multiple integrals. *International Journal for Numerical Methods in Engineering*, 1971.

Appendix A

Appendix

A.1 Low-fidelity Vectors

The following are the reported low-fidelity, each vector d_k contains the X,Y and Z displacement vectors (row-wise) of the nodes numbered in figure 4.5. The index k corresponds to the application of the $k-th$ load, as indicated in 4.4

```
%Low Fidelity Vectors
d1=[4.10E-01 ; -1.96E+00 ; -1.20E-02 ;
4.15E-01 ; -1.91E+00 ; -1.09E-02 ;
4.18E-01 ; -1.86E+00 ; -1.07E-02 ;
4.21E-01 ; -1.80E+00 ; -1.05E-02 ;
4.25E-01 ; -1.74E+00 ; -1.05E-02 ;
4.28E-01 ; -1.68E+00 ; -9.77E-03 ;
4.27E-01 ; -1.68E+00 ; 1.19E-02 ;
4.24E-01 ; -1.75E+00 ; 1.23E-02 ;
4.21E-01 ; -1.80E+00 ; 1.26E-02 ;
4.18E-01 ; -1.86E+00 ; 1.23E-02 ;
4.15E-01 ; -1.91E+00 ; 1.26E-02 ;
4.10E-01 ; -1.97E+00 ; 1.43E-02];
d2=[3.86E+01 ; -1.89E+02 ; -1.19E+00 ;
3.91E+01 ; -1.84E+02 ; -1.09E+00 ;
3.95E+01 ; -1.79E+02 ; -1.08E+00 ;
3.98E+01 ; -1.74E+02 ; -1.06E+00 ;
4.01E+01 ; -1.69E+02 ; -1.06E+00 ;
4.05E+01 ; -1.63E+02 ; -9.91E-01 ;
```

```
4.04E+01 ; -1.63E+02 ; 1.23E+00 ;
4.01E+01 ; -1.69E+02 ; 1.26E+00 ;
3.98E+01 ; -1.75E+02 ; 1.29E+00 ;
3.94E+01 ; -1.80E+02 ; 1.25E+00 ;
3.91E+01 ; -1.85E+02 ; 1.29E+00 ;
3.86E+01 ; -1.90E+02 ; 1.45E+00];
d3=[4.32E+01 ; -2.03E+02 ; -1.21E+00 ;
4.36E+01 ; -1.97E+02 ; -1.09E+00 ;
4.39E+01 ; -1.91E+02 ; -1.07E+00 ;
4.42E+01 ; -1.85E+02 ; -1.04E+00 ;
4.45E+01 ; -1.79E+02 ; -1.03E+00 ;
4.47E+01 ; -1.73E+02 ; -9.58E-01 ;
4.47E+01 ; -1.73E+02 ; 1.14E+00 ;
4.44E+01 ; -1.79E+02 ; 1.18E+00 ;
4.41E+01 ; -1.85E+02 ; 1.22E+00 ;
4.39E+01 ; -1.91E+02 ; 1.19E+00 ;
4.36E+01 ; -1.97E+02 ; 1.23E+00 ;
4.31E+01 ; -2.03E+02 ; 1.40E+00];
d4=[4.17E+01 ; -2.07E+02 ; -5.82E+00 ;
4.22E+01 ; -2.01E+02 ; -5.65E+00 ;
4.26E+01 ; -1.96E+02 ; -5.59E+00 ;
4.29E+01 ; -1.90E+02 ; -5.55E+00 ;
4.32E+01 ; -1.84E+02 ; -5.51E+00 ;
4.36E+01 ; -1.78E+02 ; -5.39E+00 ;
4.17E+01 ; -1.58E+02 ; -3.16E+00 ;
4.13E+01 ; -1.64E+02 ; -3.16E+00 ;
4.11E+01 ; -1.70E+02 ; -3.16E+00 ;
4.08E+01 ; -1.76E+02 ; -3.22E+00 ;
4.04E+01 ; -1.81E+02 ; -3.23E+00 ;
4.00E+01 ; -1.86E+02 ; -3.13E+00];
d5=[3.94E+01 ; -2.00E+02 ; -5.75E+00 ;
3.99E+01 ; -1.95E+02 ; -5.59E+00 ;
4.03E+01 ; -1.90E+02 ; -5.55E+00 ;
4.06E+01 ; -1.84E+02 ; -5.51E+00 ;
4.10E+01 ; -1.79E+02 ; -5.49E+00 ;
4.14E+01 ; -1.73E+02 ; -5.39E+00 ;
3.96E+01 ; -1.54E+02 ; -3.10E+00 ;
3.92E+01 ; -1.59E+02 ; -3.11E+00 ;
```

```
3.89E+01 ; -1.65E+02 ; -3.11E+00 ;
3.86E+01 ; -1.70E+02 ; -3.17E+00 ;
3.82E+01 ; -1.75E+02 ; -3.18E+00 ;
3.78E+01 ; -1.80E+02 ; -3.08E+00];
d6=[4.41E+01 ; -2.13E+02 ; -5.87E+00 ;
4.45E+01 ; -2.08E+02 ; -5.69E+00 ;
4.49E+01 ; -2.02E+02 ; -5.62E+00 ;
4.51E+01 ; -1.96E+02 ; -5.56E+00 ;
4.54E+01 ; -1.89E+02 ; -5.51E+00 ;
4.57E+01 ; -1.83E+02 ; -5.38E+00 ;
4.37E+01 ; -1.63E+02 ; -3.23E+00 ;
4.34E+01 ; -1.69E+02 ; -3.24E+00 ;
4.32E+01 ; -1.75E+02 ; -3.24E+00 ;
4.29E+01 ; -1.81E+02 ; -3.29E+00 ;
4.26E+01 ; -1.87E+02 ; -3.30E+00 ;
4.22E+01 ; -1.92E+02 ; -3.20E+00];
d7=[4.01E+01 ; -1.86E+02 ; 3.36E+00 ;
4.05E+01 ; -1.81E+02 ; 3.42E+00 ;
4.08E+01 ; -1.75E+02 ; 3.38E+00 ;
4.11E+01 ; -1.70E+02 ; 3.38E+00 ;
4.14E+01 ; -1.64E+02 ; 3.35E+00 ;
4.17E+01 ; -1.58E+02 ; 3.38E+00 ;
4.35E+01 ; -1.78E+02 ; 5.60E+00 ;
4.32E+01 ; -1.84E+02 ; 5.69E+00 ;
4.29E+01 ; -1.90E+02 ; 5.76E+00 ;
4.26E+01 ; -1.96E+02 ; 5.75E+00 ;
4.22E+01 ; -2.02E+02 ; 5.84E+00 ;
4.17E+01 ; -2.07E+02 ; 6.07E+00];
d8=[3.78E+01 ; -1.79E+02 ; 3.33E+00 ;
3.83E+01 ; -1.74E+02 ; 3.39E+00 ;
3.86E+01 ; -1.69E+02 ; 3.35E+00 ;
3.89E+01 ; -1.64E+02 ; 3.35E+00 ;
3.93E+01 ; -1.59E+02 ; 3.32E+00 ;
3.96E+01 ; -1.53E+02 ; 3.34E+00 ;
4.13E+01 ; -1.73E+02 ; 5.63E+00 ;
4.09E+01 ; -1.79E+02 ; 5.70E+00 ;
4.06E+01 ; -1.85E+02 ; 5.75E+00 ;
4.03E+01 ; -1.90E+02 ; 5.72E+00 ;
```

```
3.99E+01 ; -1.95E+02 ; 5.80E+00 ;
3.94E+01 ; -2.00E+02 ; 6.01E+00];
d9=[4.23E+01 ; -1.92E+02 ; 3.42E+00 ;
4.27E+01 ; -1.87E+02 ; 3.47E+00 ;
4.30E+01 ; -1.81E+02 ; 3.44E+00 ;
4.32E+01 ; -1.75E+02 ; 3.44E+00 ;
4.35E+01 ; -1.69E+02 ; 3.41E+00 ;
4.38E+01 ; -1.63E+02 ; 3.42E+00 ;
4.56E+01 ; -1.83E+02 ; 5.59E+00 ;
4.53E+01 ; -1.89E+02 ; 5.69E+00 ;
4.51E+01 ; -1.96E+02 ; 5.77E+00 ;
4.48E+01 ; -2.02E+02 ; 5.76E+00 ;
4.45E+01 ; -2.08E+02 ; 5.85E+00 ;
4.40E+01 ; -2.14E+02 ; 6.08E+00];
d10=[4.26E+01 ; -2.17E+02 ; -1.05E+01 ;
4.31E+01 ; -2.12E+02 ; -1.03E+01 ;
4.35E+01 ; -2.06E+02 ; -1.02E+01 ;
4.38E+01 ; -2.00E+02 ; -1.01E+01 ;
4.42E+01 ; -1.94E+02 ; -1.00E+01 ;
4.45E+01 ; -1.88E+02 ; -9.84E+00 ;
4.08E+01 ; -1.49E+02 ; -7.51E+00 ;
4.04E+01 ; -1.54E+02 ; -7.56E+00 ;
4.01E+01 ; -1.60E+02 ; -7.59E+00 ;
3.99E+01 ; -1.66E+02 ; -7.67E+00 ;
3.96E+01 ; -1.71E+02 ; -7.73E+00 ;
3.92E+01 ; -1.76E+02 ; -7.69E+00];
d11=[3.39E+01 ; -1.77E+02 ; -8.73E+00 ;
3.43E+01 ; -1.72E+02 ; -8.56E+00 ;
3.46E+01 ; -1.68E+02 ; -8.48E+00 ;
3.49E+01 ; -1.64E+02 ; -8.44E+00 ;
3.52E+01 ; -1.59E+02 ; -8.40E+00 ;
3.56E+01 ; -1.54E+02 ; -8.26E+00 ;
3.26E+01 ; -1.21E+02 ; -6.23E+00 ;
3.23E+01 ; -1.26E+02 ; -6.27E+00 ;
3.20E+01 ; -1.30E+02 ; -6.29E+00 ;
3.17E+01 ; -1.34E+02 ; -6.35E+00 ;
3.15E+01 ; -1.39E+02 ; -6.40E+00 ;
3.11E+01 ; -1.43E+02 ; -6.36E+00];
```

```
d12=[4.49E+01 ; -2.24E+02 ; -1.06E+01 ;
4.54E+01 ; -2.18E+02 ; -1.03E+01 ;
4.58E+01 ; -2.12E+02 ; -1.02E+01 ;
4.61E+01 ; -2.06E+02 ; -1.01E+01 ;
4.64E+01 ; -1.99E+02 ; -1.01E+01 ;
4.67E+01 ; -1.93E+02 ; -9.87E+00 ;
4.28E+01 ; -1.53E+02 ; -7.60E+00 ;
4.25E+01 ; -1.59E+02 ; -7.65E+00 ;
4.22E+01 ; -1.65E+02 ; -7.69E+00 ;
4.20E+01 ; -1.71E+02 ; -7.77E+00 ;
4.17E+01 ; -1.77E+02 ; -7.83E+00 ;
4.13E+01 ; -1.82E+02 ; -7.80E+00];
d13=[3.92E+01 ; -1.76E+02 ; 7.90E+00 ;
3.96E+01 ; -1.71E+02 ; 7.90E+00 ;
3.99E+01 ; -1.65E+02 ; 7.81E+00 ;
4.02E+01 ; -1.60E+02 ; 7.80E+00 ;
4.05E+01 ; -1.54E+02 ; 7.73E+00 ;
4.08E+01 ; -1.48E+02 ; 7.70E+00 ;
4.45E+01 ; -1.88E+02 ; 1.01E+01 ;
4.41E+01 ; -1.95E+02 ; 1.02E+01 ;
4.38E+01 ; -2.01E+02 ; 1.03E+01 ;
4.35E+01 ; -2.06E+02 ; 1.03E+01 ;
4.31E+01 ; -2.12E+02 ; 1.04E+01 ;
4.26E+01 ; -2.17E+02 ; 1.07E+01];
d14=[3.92E+01 ; -1.76E+02 ; 7.90E+00 ;
3.96E+01 ; -1.71E+02 ; 7.90E+00 ;
3.99E+01 ; -1.65E+02 ; 7.81E+00 ;
4.02E+01 ; -1.60E+02 ; 7.80E+00 ;
4.05E+01 ; -1.54E+02 ; 7.73E+00 ;
4.08E+01 ; -1.48E+02 ; 7.70E+00 ;
4.45E+01 ; -1.88E+02 ; 1.01E+01 ;
4.41E+01 ; -1.95E+02 ; 1.02E+01 ;
4.38E+01 ; -2.01E+02 ; 1.03E+01 ;
4.35E+01 ; -2.06E+02 ; 1.03E+01 ;
4.31E+01 ; -2.12E+02 ; 1.04E+01 ;
4.26E+01 ; -2.17E+02 ; 1.07E+01];
d15=[4.14E+01 ; -1.82E+02 ; 8.00E+00 ;
4.18E+01 ; -1.76E+02 ; 8.00E+00 ;
```

```
4.21E+01 ; -1.71E+02 ; 7.91E+00 ;
4.23E+01 ; -1.65E+02 ; 7.89E+00 ;
4.26E+01 ; -1.59E+02 ; 7.82E+00 ;
4.29E+01 ; -1.53E+02 ; 7.78E+00 ;
4.66E+01 ; -1.93E+02 ; 1.01E+01 ;
4.63E+01 ; -2.00E+02 ; 1.02E+01 ;
4.61E+01 ; -2.06E+02 ; 1.03E+01 ;
4.58E+01 ; -2.12E+02 ; 1.04E+01 ;
4.54E+01 ; -2.18E+02 ; 1.05E+01 ;
4.49E+01 ; -2.24E+02 ; 1.08E+01];
d16=[4.34E+01 ; -2.28E+02 ; -1.52E+01 ;
4.39E+01 ; -2.22E+02 ; -1.49E+01 ;
4.44E+01 ; -2.17E+02 ; -1.48E+01 ;
4.47E+01 ; -2.11E+02 ; -1.47E+01 ;
4.51E+01 ; -2.05E+02 ; -1.46E+01 ;
4.54E+01 ; -1.98E+02 ; -1.44E+01 ;
3.99E+01 ; -1.39E+02 ; -1.18E+01 ;
3.95E+01 ; -1.45E+02 ; -1.19E+01 ;
3.92E+01 ; -1.50E+02 ; -1.20E+01 ;
3.89E+01 ; -1.56E+02 ; -1.21E+01 ;
3.87E+01 ; -1.61E+02 ; -1.22E+01 ;
3.83E+01 ; -1.66E+02 ; -1.22E+01];
d17=[4.10E+01 ; -2.20E+02 ; -1.51E+01 ;
4.15E+01 ; -2.15E+02 ; -1.48E+01 ;
4.20E+01 ; -2.10E+02 ; -1.47E+01 ;
4.23E+01 ; -2.05E+02 ; -1.46E+01 ;
4.28E+01 ; -1.99E+02 ; -1.45E+01 ;
4.31E+01 ; -1.93E+02 ; -1.43E+01 ;
3.78E+01 ; -1.34E+02 ; -1.17E+01 ;
3.75E+01 ; -1.40E+02 ; -1.18E+01 ;
3.71E+01 ; -1.45E+02 ; -1.18E+01 ;
3.68E+01 ; -1.50E+02 ; -1.19E+01 ;
3.65E+01 ; -1.55E+02 ; -1.20E+01 ;
3.61E+01 ; -1.59E+02 ; -1.21E+01];
d18=[4.58E+01 ; -2.35E+02 ; -1.53E+01 ;
4.64E+01 ; -2.29E+02 ; -1.50E+01 ;
4.68E+01 ; -2.23E+02 ; -1.49E+01 ;
4.71E+01 ; -2.17E+02 ; -1.48E+01 ;
```

```
4.74E+01 ; -2.10E+02 ; -1.47E+01 ;
4.77E+01 ; -2.03E+02 ; -1.44E+01 ;
4.19E+01 ; -1.43E+02 ; -1.19E+01 ;
4.16E+01 ; -1.49E+02 ; -1.20E+01 ;
4.13E+01 ; -1.55E+02 ; -1.21E+01 ;
4.10E+01 ; -1.61E+02 ; -1.22E+01 ;
4.08E+01 ; -1.66E+02 ; -1.23E+01 ;
4.04E+01 ; -1.72E+02 ; -1.23E+01];
d19=[3.84E+01 ; -1.66E+02 ; 1.24E+01 ;
3.87E+01 ; -1.61E+02 ; 1.24E+01 ;
3.91E+01 ; -1.55E+02 ; 1.22E+01 ;
3.93E+01 ; -1.50E+02 ; 1.22E+01 ;
3.97E+01 ; -1.45E+02 ; 1.21E+01 ;
4.00E+01 ; -1.39E+02 ; 1.20E+01 ;
4.54E+01 ; -1.99E+02 ; 1.46E+01 ;
4.50E+01 ; -2.05E+02 ; 1.48E+01 ;
4.47E+01 ; -2.11E+02 ; 1.49E+01 ;
4.44E+01 ; -2.17E+02 ; 1.49E+01 ;
4.40E+01 ; -2.23E+02 ; 1.51E+01 ;
4.34E+01 ; -2.28E+02 ; 1.54E+01];
d20=[3.62E+01 ; -1.59E+02 ; 1.23E+01 ;
3.66E+01 ; -1.55E+02 ; 1.22E+01 ;
3.69E+01 ; -1.50E+02 ; 1.21E+01 ;
3.72E+01 ; -1.45E+02 ; 1.21E+01 ;
3.76E+01 ; -1.40E+02 ; 1.20E+01 ;
3.79E+01 ; -1.34E+02 ; 1.19E+01 ;
4.31E+01 ; -1.93E+02 ; 1.46E+01 ;
4.27E+01 ; -2.00E+02 ; 1.47E+01 ;
4.24E+01 ; -2.05E+02 ; 1.48E+01 ;
4.20E+01 ; -2.11E+02 ; 1.48E+01 ;
4.16E+01 ; -2.16E+02 ; 1.50E+01 ;
4.10E+01 ; -2.21E+02 ; 1.53E+01];
d21=[4.05E+01 ; -1.72E+02 ; 1.26E+01 ;
4.08E+01 ; -1.66E+02 ; 1.25E+01 ;
4.11E+01 ; -1.61E+02 ; 1.24E+01 ;
4.14E+01 ; -1.55E+02 ; 1.23E+01 ;
4.17E+01 ; -1.49E+02 ; 1.22E+01 ;
4.20E+01 ; -1.43E+02 ; 1.21E+01 ;
```

```
4.77E+01 ; -2.03E+02 ; 1.46E+01 ;
4.73E+01 ; -2.10E+02 ; 1.48E+01 ;
4.71E+01 ; -2.17E+02 ; 1.50E+01 ;
4.68E+01 ; -2.23E+02 ; 1.50E+01 ;
4.64E+01 ; -2.29E+02 ; 1.52E+01 ;
4.58E+01 ; -2.35E+02 ; 1.56E+01];
d22=[4.54E+01 ; -2.09E+02 ; -1.21E+00 ;
4.58E+01 ; -2.03E+02 ; -1.09E+00 ;
4.61E+01 ; -1.97E+02 ; -1.07E+00 ;
4.63E+01 ; -1.90E+02 ; -1.04E+00 ;
4.66E+01 ; -1.84E+02 ; -1.02E+00 ;
4.68E+01 ; -1.77E+02 ; -9.42E-01 ;
4.68E+01 ; -1.77E+02 ; 1.09E+00 ;
4.65E+01 ; -1.84E+02 ; 1.14E+00 ;
4.63E+01 ; -1.91E+02 ; 1.19E+00 ;
4.61E+01 ; -1.97E+02 ; 1.17E+00 ;
4.58E+01 ; -2.03E+02 ; 1.21E+00 ;
4.54E+01 ; -2.09E+02 ; 1.39E+00];
d23=[4.64E+01 ; -2.20E+02 ; -5.89E+00 ;
4.68E+01 ; -2.14E+02 ; -5.70E+00 ;
4.71E+01 ; -2.07E+02 ; -5.62E+00 ;
4.73E+01 ; -2.01E+02 ; -5.56E+00 ;
4.76E+01 ; -1.94E+02 ; -5.51E+00 ;
4.78E+01 ; -1.87E+02 ; -5.37E+00 ;
4.58E+01 ; -1.67E+02 ; -3.32E+00 ;
4.55E+01 ; -1.74E+02 ; -3.32E+00 ;
4.53E+01 ; -1.80E+02 ; -3.32E+00 ;
4.51E+01 ; -1.87E+02 ; -3.37E+00 ;
4.48E+01 ; -1.93E+02 ; -3.38E+00 ;
4.44E+01 ; -1.99E+02 ; -3.28E+00];
d24=[4.45E+01 ; -1.98E+02 ; 3.47E+00 ;
4.49E+01 ; -1.92E+02 ; 3.52E+00 ;
4.52E+01 ; -1.86E+02 ; 3.49E+00 ;
4.53E+01 ; -1.80E+02 ; 3.49E+00 ;
4.56E+01 ; -1.74E+02 ; 3.46E+00 ;
4.58E+01 ; -1.67E+02 ; 3.48E+00 ;
4.77E+01 ; -1.87E+02 ; 5.54E+00 ;
4.75E+01 ; -1.94E+02 ; 5.65E+00 ;
```

```
4.73E+01 ; -2.01E+02 ; 5.74E+00 ;
4.71E+01 ; -2.07E+02 ; 5.74E+00 ;
4.68E+01 ; -2.14E+02 ; 5.84E+00 ;
4.63E+01 ; -2.20E+02 ; 6.09E+00];
d25=[3.64E+01 ; -1.82E+02 ; -1.18E+00 ;
3.69E+01 ; -1.78E+02 ; -1.07E+00 ;
3.72E+01 ; -1.73E+02 ; -1.07E+00 ;
3.75E+01 ; -1.68E+02 ; -1.06E+00 ;
3.79E+01 ; -1.63E+02 ; -1.06E+00 ;
3.83E+01 ; -1.58E+02 ; -9.96E-01 ;
3.83E+01 ; -1.58E+02 ; 1.28E+00 ;
3.79E+01 ; -1.64E+02 ; 1.31E+00 ;
3.75E+01 ; -1.69E+02 ; 1.33E+00 ;
3.72E+01 ; -1.73E+02 ; 1.29E+00 ;
3.69E+01 ; -1.78E+02 ; 1.31E+00 ;
3.64E+01 ; -1.83E+02 ; 1.47E+00];
d26=[3.72E+01 ; -1.92E+02 ; -5.69E+00 ;
3.76E+01 ; -1.88E+02 ; -5.54E+00 ;
3.81E+01 ; -1.83E+02 ; -5.50E+00 ;
3.84E+01 ; -1.78E+02 ; -5.47E+00 ;
3.88E+01 ; -1.73E+02 ; -5.45E+00 ;
3.92E+01 ; -1.68E+02 ; -5.35E+00 ;
3.74E+01 ; -1.49E+02 ; -3.05E+00 ;
3.70E+01 ; -1.54E+02 ; -3.06E+00 ;
3.67E+01 ; -1.59E+02 ; -3.06E+00 ;
3.64E+01 ; -1.64E+02 ; -3.12E+00 ;
3.60E+01 ; -1.68E+02 ; -3.13E+00 ;
3.56E+01 ; -1.73E+02 ; -3.03E+00];
d27=[3.56E+01 ; -1.72E+02 ; 3.29E+00 ;
3.61E+01 ; -1.68E+02 ; 3.35E+00 ;
3.64E+01 ; -1.63E+02 ; 3.31E+00 ;
3.67E+01 ; -1.58E+02 ; 3.30E+00 ;
3.71E+01 ; -1.53E+02 ; 3.27E+00 ;
3.75E+01 ; -1.48E+02 ; 3.29E+00 ;
3.91E+01 ; -1.68E+02 ; 5.63E+00 ;
3.87E+01 ; -1.74E+02 ; 5.69E+00 ;
3.84E+01 ; -1.79E+02 ; 5.74E+00 ;
3.80E+01 ; -1.84E+02 ; 5.71E+00 ;
```

```
3.77E+01 ; -1.88E+02 ; 5.77E+00 ;
3.72E+01 ; -1.93E+02 ; 5.98E+00];
d28=[4.36E+01 ; -1.88E+02 ; 8.09E+00 ;
4.39E+01 ; -1.82E+02 ; 8.08E+00 ;
4.42E+01 ; -1.76E+02 ; 7.99E+00 ;
4.44E+01 ; -1.70E+02 ; 7.96E+00 ;
4.47E+01 ; -1.64E+02 ; 7.89E+00 ;
4.49E+01 ; -1.57E+02 ; 7.85E+00 ;
4.88E+01 ; -1.97E+02 ; 1.00E+01 ;
4.85E+01 ; -2.05E+02 ; 1.02E+01 ;
4.83E+01 ; -2.11E+02 ; 1.03E+01 ;
4.81E+01 ; -2.18E+02 ; 1.04E+01 ;
4.78E+01 ; -2.24E+02 ; 1.05E+01 ;
4.73E+01 ; -2.31E+02 ; 1.09E+01];
d29=[3.49E+01 ; -1.62E+02 ; 7.74E+00 ;
3.53E+01 ; -1.58E+02 ; 7.74E+00 ;
3.56E+01 ; -1.54E+02 ; 7.66E+00 ;
3.59E+01 ; -1.49E+02 ; 7.65E+00 ;
3.63E+01 ; -1.44E+02 ; 7.59E+00 ;
3.67E+01 ; -1.39E+02 ; 7.56E+00 ;
4.00E+01 ; -1.78E+02 ; 1.00E+01 ;
3.95E+01 ; -1.84E+02 ; 1.01E+01 ;
3.92E+01 ; -1.89E+02 ; 1.02E+01 ;
3.88E+01 ; -1.94E+02 ; 1.02E+01 ;
3.84E+01 ; -1.99E+02 ; 1.03E+01 ;
3.79E+01 ; -2.03E+02 ; 1.06E+01];
d30=[4.73E+01 ; -2.31E+02 ; -1.06E+01 ;
4.78E+01 ; -2.24E+02 ; -1.04E+01 ;
4.81E+01 ; -2.18E+02 ; -1.03E+01 ;
4.83E+01 ; -2.11E+02 ; -1.02E+01 ;
4.86E+01 ; -2.04E+02 ; -1.01E+01 ;
4.88E+01 ; -1.97E+02 ; -9.85E+00 ;
4.48E+01 ; -1.57E+02 ; -7.70E+00 ;
4.45E+01 ; -1.64E+02 ; -7.76E+00 ;
4.43E+01 ; -1.70E+02 ; -7.80E+00 ;
4.41E+01 ; -1.76E+02 ; -7.88E+00 ;
4.39E+01 ; -1.82E+02 ; -7.94E+00 ;
4.35E+01 ; -1.88E+02 ; -7.92E+00];
```

A.2 High-fidelity Vectors

The following are the reported high-fidelity, each vector h_k contains the X,Y and Z displacement vectors (row-wise) of the nodes numbered in figure 4.5. The index k corresponds to the application of the $k-th$ load, as indicated in 4.4

```
%High Fidelity Vectors
h1=[4.68E+01 ; -2.21E+02 ; -1.40E+00 ;
4.72E+01 ; -2.15E+02 ; -1.15E+00 ;
4.76E+01 ; -2.09E+02 ; -1.17E+00 ;
4.78E+01 ; -2.03E+02 ; -1.30E+00 ;
4.81E+01 ; -1.96E+02 ; -1.28E+00 ;
4.84E+01 ; -1.89E+02 ; -1.22E+00 ;
4.83E+01 ; -1.89E+02 ; 1.34E+00 ;
4.81E+01 ; -1.96E+02 ; 1.39E+00 ;
4.78E+01 ; -2.03E+02 ; 1.41E+00 ;
4.76E+01 ; -2.09E+02 ; 1.27E+00 ;
4.72E+01 ; -2.15E+02 ; 1.26E+00 ;
4.67E+01 ; -2.21E+02 ; 1.52E+00 ];
h2=[4.42E+01 ; -2.14E+02 ; -1.39E+00 ;
4.47E+01 ; -2.08E+02 ; -1.15E+00 ;
4.51E+01 ; -2.02E+02 ; -1.17E+00 ;
4.53E+01 ; -1.96E+02 ; -1.30E+00 ;
4.56E+01 ; -1.90E+02 ; -1.29E+00 ;
4.59E+01 ; -1.84E+02 ; -1.24E+00 ;
4.59E+01 ; -1.84E+02 ; 1.38E+00 ;
4.56E+01 ; -1.90E+02 ; 1.43E+00 ;
4.53E+01 ; -1.96E+02 ; 1.45E+00 ;
4.50E+01 ; -2.02E+02 ; 1.30E+00 ;
4.46E+01 ; -2.08E+02 ; 1.29E+00 ;
4.42E+01 ; -2.14E+02 ; 1.54E+00 ];
h3=[4.94E+01 ; -2.29E+02 ; -1.41E+00 ;
4.98E+01 ; -2.22E+02 ; -1.15E+00 ;
5.01E+01 ; -2.16E+02 ; -1.16E+00 ;
5.03E+01 ; -2.09E+02 ; -1.29E+00 ;
5.06E+01 ; -2.02E+02 ; -1.26E+00 ;
5.08E+01 ; -1.94E+02 ; -1.20E+00 ;
```

```
5.07E+01 ; -1.94E+02 ; 1.27E+00 ;
5.05E+01 ; -2.02E+02 ; 1.33E+00 ;
5.03E+01 ; -2.09E+02 ; 1.37E+00 ;
5.01E+01 ; -2.16E+02 ; 1.23E+00 ;
4.98E+01 ; -2.22E+02 ; 1.22E+00 ;
4.93E+01 ; -2.29E+02 ; 1.49E+00 ];
h4=[4.77E+01 ; -2.33E+02 ; -6.89E+00 ;
4.82E+01 ; -2.27E+02 ; -6.55E+00 ;
4.86E+01 ; -2.21E+02 ; -6.51E+00 ;
4.88E+01 ; -2.14E+02 ; -6.64E+00 ;
4.91E+01 ; -2.08E+02 ; -6.58E+00 ;
4.94E+01 ; -2.01E+02 ; -6.46E+00 ;
4.74E+01 ; -1.78E+02 ; -3.86E+00 ;
4.71E+01 ; -1.85E+02 ; -3.87E+00 ;
4.68E+01 ; -1.91E+02 ; -3.88E+00 ;
4.66E+01 ; -1.97E+02 ; -4.02E+00 ;
4.62E+01 ; -2.03E+02 ; -4.09E+00 ;
4.58E+01 ; -2.09E+02 ; -3.92E+00 ];
h5=[4.51E+01 ; -2.25E+02 ; -6.81E+00 ;
4.56E+01 ; -2.20E+02 ; -6.49E+00 ;
4.60E+01 ; -2.14E+02 ; -6.46E+00 ;
4.62E+01 ; -2.08E+02 ; -6.60E+00 ;
4.65E+01 ; -2.02E+02 ; -6.56E+00 ;
4.69E+01 ; -1.95E+02 ; -6.45E+00 ;
4.50E+01 ; -1.72E+02 ; -3.78E+00 ;
4.46E+01 ; -1.79E+02 ; -3.79E+00 ;
4.43E+01 ; -1.85E+02 ; -3.80E+00 ;
4.41E+01 ; -1.91E+02 ; -3.94E+00 ;
4.37E+01 ; -1.96E+02 ; -4.02E+00 ;
4.33E+01 ; -2.02E+02 ; -3.85E+00 ];
h6=[5.03E+01 ; -2.41E+02 ; -6.95E+00 ;
5.08E+01 ; -2.34E+02 ; -6.60E+00 ;
5.12E+01 ; -2.28E+02 ; -6.54E+00 ;
5.13E+01 ; -2.21E+02 ; -6.67E+00 ;
5.16E+01 ; -2.14E+02 ; -6.60E+00 ;
5.18E+01 ; -2.06E+02 ; -6.47E+00 ;
4.97E+01 ; -1.83E+02 ; -3.95E+00 ;
4.95E+01 ; -1.90E+02 ; -3.96E+00 ;
```

```
4.92E+01 ; -1.97E+02 ; -3.97E+00 ;
4.91E+01 ; -2.04E+02 ; -4.10E+00 ;
4.87E+01 ; -2.10E+02 ; -4.18E+00 ;
4.83E+01 ; -2.17E+02 ; -4.00E+00 ];
h7=[4.59E+01 ; -2.09E+02 ; 4.04E+00 ;
4.63E+01 ; -2.03E+02 ; 4.20E+00 ;
4.66E+01 ; -1.97E+02 ; 4.12E+00 ;
4.69E+01 ; -1.91E+02 ; 3.99E+00 ;
4.71E+01 ; -1.85E+02 ; 3.97E+00 ;
4.74E+01 ; -1.78E+02 ; 3.97E+00 ;
4.93E+01 ; -2.01E+02 ; 6.58E+00 ;
4.90E+01 ; -2.08E+02 ; 6.69E+00 ;
4.88E+01 ; -2.15E+02 ; 6.76E+00 ;
4.86E+01 ; -2.21E+02 ; 6.61E+00 ;
4.82E+01 ; -2.27E+02 ; 6.66E+00 ;
4.77E+01 ; -2.33E+02 ; 7.01E+00 ];
h8=[4.33E+01 ; -2.02E+02 ; 4.00E+00 ;
4.38E+01 ; -1.96E+02 ; 4.16E+00 ;
4.41E+01 ; -1.91E+02 ; 4.08E+00 ;
4.44E+01 ; -1.85E+02 ; 3.95E+00 ;
4.47E+01 ; -1.79E+02 ; 3.93E+00 ;
4.50E+01 ; -1.72E+02 ; 3.92E+00 ;
4.69E+01 ; -1.95E+02 ; 6.60E+00 ;
4.65E+01 ; -2.02E+02 ; 6.70E+00 ;
4.62E+01 ; -2.08E+02 ; 6.75E+00 ;
4.60E+01 ; -2.14E+02 ; 6.60E+00 ;
4.56E+01 ; -2.20E+02 ; 6.64E+00 ;
4.51E+01 ; -2.26E+02 ; 6.97E+00 ];
h9=[4.84E+01 ; -2.17E+02 ; 4.09E+00 ;
4.88E+01 ; -2.10E+02 ; 4.25E+00 ;
4.91E+01 ; -2.04E+02 ; 4.17E+00 ;
4.93E+01 ; -1.97E+02 ; 4.05E+00 ;
4.95E+01 ; -1.90E+02 ; 4.03E+00 ;
4.98E+01 ; -1.83E+02 ; 4.03E+00 ;
5.18E+01 ; -2.06E+02 ; 6.55E+00 ;
5.15E+01 ; -2.14E+02 ; 6.67E+00 ;
5.13E+01 ; -2.21E+02 ; 6.75E+00 ;
5.11E+01 ; -2.28E+02 ; 6.61E+00 ;
```

```
5.08E+01 ; -2.34E+02 ; 6.67E+00 ;
5.03E+01 ; -2.41E+02 ; 7.03E+00 ];
h10=[4.86E+01 ; -2.45E+02 ; -1.24E+01 ;
4.91E+01 ; -2.39E+02 ; -1.20E+01 ;
4.96E+01 ; -2.33E+02 ; -1.19E+01 ;
4.98E+01 ; -2.26E+02 ; -1.20E+01 ;
5.01E+01 ; -2.20E+02 ; -1.19E+01 ;
5.04E+01 ; -2.12E+02 ; -1.18E+01 ;
4.64E+01 ; -1.67E+02 ; -9.02E+00 ;
4.61E+01 ; -1.73E+02 ; -9.09E+00 ;
4.58E+01 ; -1.80E+02 ; -9.14E+00 ;
4.56E+01 ; -1.86E+02 ; -9.27E+00 ;
4.53E+01 ; -1.92E+02 ; -9.41E+00 ;
4.49E+01 ; -1.98E+02 ; -9.33E+00 ];
h11=[4.59E+01 ; -2.37E+02 ; -1.23E+01 ;
4.65E+01 ; -2.32E+02 ; -1.19E+01 ;
4.69E+01 ; -2.26E+02 ; -1.18E+01 ;
4.72E+01 ; -2.20E+02 ; -1.20E+01 ;
4.75E+01 ; -2.13E+02 ; -1.19E+01 ;
4.78E+01 ; -2.07E+02 ; -1.17E+01 ;
4.40E+01 ; -1.61E+02 ; -8.91E+00 ;
4.37E+01 ; -1.67E+02 ; -8.97E+00 ;
4.34E+01 ; -1.73E+02 ; -9.02E+00 ;
4.31E+01 ; -1.79E+02 ; -9.16E+00 ;
4.28E+01 ; -1.85E+02 ; -9.29E+00 ;
4.24E+01 ; -1.90E+02 ; -9.20E+00 ];
h12=[5.13E+01 ; -2.53E+02 ; -1.25E+01 ;
5.18E+01 ; -2.46E+02 ; -1.21E+01 ;
5.22E+01 ; -2.40E+02 ; -1.20E+01 ;
5.24E+01 ; -2.33E+02 ; -1.21E+01 ;
5.26E+01 ; -2.25E+02 ; -1.20E+01 ;
5.29E+01 ; -2.18E+02 ; -1.18E+01 ;
4.87E+01 ; -1.72E+02 ; -9.13E+00 ;
4.85E+01 ; -1.79E+02 ; -9.20E+00 ;
4.82E+01 ; -1.85E+02 ; -9.26E+00 ;
4.80E+01 ; -1.92E+02 ; -9.39E+00 ;
4.77E+01 ; -1.98E+02 ; -9.54E+00 ;
4.74E+01 ; -2.05E+02 ; -9.45E+00 ];
```

```
h13=[4.49E+01 ; -1.98E+02 ; 9.44E+00 ;
4.53E+01 ; -1.92E+02 ; 9.52E+00 ;
4.57E+01 ; -1.86E+02 ; 9.37E+00 ;
4.59E+01 ; -1.80E+02 ; 9.25E+00 ;
4.62E+01 ; -1.73E+02 ; 9.19E+00 ;
4.65E+01 ; -1.66E+02 ; 9.13E+00 ;
5.03E+01 ; -2.12E+02 ; 1.19E+01 ;
5.00E+01 ; -2.20E+02 ; 1.21E+01 ;
4.98E+01 ; -2.26E+02 ; 1.22E+01 ;
4.95E+01 ; -2.33E+02 ; 1.20E+01 ;
4.91E+01 ; -2.39E+02 ; 1.21E+01 ;
4.86E+01 ; -2.45E+02 ; 1.25E+01 ];
h14=[4.24E+01 ; -1.90E+02 ; 9.34E+00 ;
4.28E+01 ; -1.85E+02 ; 9.43E+00 ;
4.32E+01 ; -1.79E+02 ; 9.28E+00 ;
4.35E+01 ; -1.73E+02 ; 9.16E+00 ;
4.38E+01 ; -1.67E+02 ; 9.10E+00 ;
4.41E+01 ; -1.61E+02 ; 9.04E+00 ;
4.78E+01 ; -2.07E+02 ; 1.19E+01 ;
4.75E+01 ; -2.14E+02 ; 1.20E+01 ;
4.71E+01 ; -2.20E+02 ; 1.21E+01 ;
4.69E+01 ; -2.26E+02 ; 1.19E+01 ;
4.65E+01 ; -2.32E+02 ; 1.20E+01 ;
4.59E+01 ; -2.38E+02 ; 1.24E+01 ];
h15=[4.74E+01 ; -2.05E+02 ; 9.54E+00 ;
4.78E+01 ; -1.98E+02 ; 9.61E+00 ;
4.81E+01 ; -1.92E+02 ; 9.46E+00 ;
4.83E+01 ; -1.85E+02 ; 9.34E+00 ;
4.85E+01 ; -1.79E+02 ; 9.27E+00 ;
4.88E+01 ; -1.72E+02 ; 9.21E+00 ;
5.28E+01 ; -2.18E+02 ; 1.19E+01 ;
5.26E+01 ; -2.25E+02 ; 1.21E+01 ;
5.24E+01 ; -2.33E+02 ; 1.22E+01 ;
5.22E+01 ; -2.40E+02 ; 1.21E+01 ;
5.18E+01 ; -2.47E+02 ; 1.22E+01 ;
5.13E+01 ; -2.53E+02 ; 1.26E+01 ];
h16=[4.95E+01 ; -2.58E+02 ; -1.80E+01 ;
5.01E+01 ; -2.51E+02 ; -1.75E+01 ;
```

```
5.06E+01 ; -2.45E+02 ; -1.74E+01 ;
5.08E+01 ; -2.38E+02 ; -1.75E+01 ;
5.11E+01 ; -2.32E+02 ; -1.74E+01 ;
5.14E+01 ; -2.24E+02 ; -1.71E+01 ;
4.54E+01 ; -1.55E+02 ; -1.41E+01 ;
4.51E+01 ; -1.62E+02 ; -1.43E+01 ;
4.49E+01 ; -1.68E+02 ; -1.44E+01 ;
4.46E+01 ; -1.74E+02 ; -1.45E+01 ;
4.43E+01 ; -1.80E+02 ; -1.47E+01 ;
4.39E+01 ; -1.86E+02 ; -1.47E+01 ];
h17=[4.68E+01 ; -2.49E+02 ; -1.78E+01 ;
4.74E+01 ; -2.44E+02 ; -1.74E+01 ;
4.78E+01 ; -2.38E+02 ; -1.72E+01 ;
4.81E+01 ; -2.32E+02 ; -1.74E+01 ;
4.84E+01 ; -2.25E+02 ; -1.73E+01 ;
4.88E+01 ; -2.18E+02 ; -1.71E+01 ;
4.31E+01 ; -1.50E+02 ; -1.40E+01 ;
4.28E+01 ; -1.56E+02 ; -1.41E+01 ;
4.25E+01 ; -1.62E+02 ; -1.42E+01 ;
4.22E+01 ; -1.68E+02 ; -1.43E+01 ;
4.19E+01 ; -1.73E+02 ; -1.45E+01 ;
4.15E+01 ; -1.79E+02 ; -1.45E+01 ];
h18=[5.23E+01 ; -2.66E+02 ; -1.82E+01 ;
5.28E+01 ; -2.59E+02 ; -1.77E+01 ;
5.33E+01 ; -2.52E+02 ; -1.75E+01 ;
5.34E+01 ; -2.45E+02 ; -1.76E+01 ;
5.37E+01 ; -2.37E+02 ; -1.74E+01 ;
5.39E+01 ; -2.30E+02 ; -1.72E+01 ;
4.77E+01 ; -1.60E+02 ; -1.43E+01 ;
4.75E+01 ; -1.67E+02 ; -1.44E+01 ;
4.72E+01 ; -1.74E+02 ; -1.45E+01 ;
4.70E+01 ; -1.80E+02 ; -1.47E+01 ;
4.67E+01 ; -1.87E+02 ; -1.49E+01 ;
4.64E+01 ; -1.93E+02 ; -1.49E+01 ];
h19=[4.40E+01 ; -1.86E+02 ; 1.48E+01 ;
4.44E+01 ; -1.80E+02 ; 1.48E+01 ;
4.47E+01 ; -1.74E+02 ; 1.46E+01 ;
4.49E+01 ; -1.68E+02 ; 1.45E+01 ;
```

```
4.52E+01 ; -1.62E+02 ; 1.44E+01 ;
4.55E+01 ; -1.55E+02 ; 1.43E+01 ;
5.14E+01 ; -2.24E+02 ; 1.73E+01 ;
5.11E+01 ; -2.32E+02 ; 1.75E+01 ;
5.08E+01 ; -2.39E+02 ; 1.76E+01 ;
5.05E+01 ; -2.45E+02 ; 1.75E+01 ;
5.01E+01 ; -2.52E+02 ; 1.76E+01 ;
4.95E+01 ; -2.58E+02 ; 1.81E+01 ];
h20=[4.16E+01 ; -1.79E+02 ; 1.47E+01 ;
4.19E+01 ; -1.73E+02 ; 1.47E+01 ;
4.23E+01 ; -1.68E+02 ; 1.45E+01 ;
4.25E+01 ; -1.62E+02 ; 1.43E+01 ;
4.29E+01 ; -1.56E+02 ; 1.42E+01 ;
4.32E+01 ; -1.50E+02 ; 1.41E+01 ;
4.88E+01 ; -2.19E+02 ; 1.72E+01 ;
4.84E+01 ; -2.25E+02 ; 1.74E+01 ;
4.81E+01 ; -2.32E+02 ; 1.75E+01 ;
4.78E+01 ; -2.38E+02 ; 1.74E+01 ;
4.74E+01 ; -2.44E+02 ; 1.75E+01 ;
4.68E+01 ; -2.50E+02 ; 1.80E+01 ];
h21=[4.64E+01 ; -1.93E+02 ; 1.50E+01 ;
4.68E+01 ; -1.87E+02 ; 1.50E+01 ;
4.71E+01 ; -1.80E+02 ; 1.47E+01 ;
4.73E+01 ; -1.74E+02 ; 1.46E+01 ;
4.76E+01 ; -1.67E+02 ; 1.45E+01 ;
4.78E+01 ; -1.60E+02 ; 1.44E+01 ;
5.39E+01 ; -2.30E+02 ; 1.73E+01 ;
5.37E+01 ; -2.38E+02 ; 1.75E+01 ;
5.34E+01 ; -2.45E+02 ; 1.77E+01 ;
5.32E+01 ; -2.52E+02 ; 1.76E+01 ;
5.28E+01 ; -2.59E+02 ; 1.78E+01 ;
5.22E+01 ; -2.66E+02 ; 1.83E+01 ];
h22=[5.20E+01 ; -2.36E+02 ; -1.41E+00 ;
5.23E+01 ; -2.29E+02 ; -1.14E+00 ;
5.27E+01 ; -2.22E+02 ; -1.15E+00 ;
5.28E+01 ; -2.15E+02 ; -1.27E+00 ;
5.30E+01 ; -2.07E+02 ; -1.24E+00 ;
5.32E+01 ; -2.00E+02 ; -1.16E+00 ;
```

```
5.31E+01 ; -1.99E+02 ; 1.20E+00 ;
5.29E+01 ; -2.07E+02 ; 1.27E+00 ;
5.27E+01 ; -2.15E+02 ; 1.31E+00 ;
5.26E+01 ; -2.22E+02 ; 1.17E+00 ;
5.23E+01 ; -2.29E+02 ; 1.17E+00 ;
5.19E+01 ; -2.36E+02 ; 1.44E+00 ];
h23=[5.30E+01 ; -2.48E+02 ; -6.98E+00 ;
5.34E+01 ; -2.41E+02 ; -6.62E+00 ;
5.37E+01 ; -2.34E+02 ; -6.55E+00 ;
5.39E+01 ; -2.27E+02 ; -6.67E+00 ;
5.41E+01 ; -2.19E+02 ; -6.59E+00 ;
5.42E+01 ; -2.11E+02 ; -6.44E+00 ;
5.20E+01 ; -1.88E+02 ; -4.04E+00 ;
5.19E+01 ; -1.95E+02 ; -4.05E+00 ;
5.17E+01 ; -2.03E+02 ; -4.06E+00 ;
5.15E+01 ; -2.10E+02 ; -4.19E+00 ;
5.12E+01 ; -2.17E+02 ; -4.26E+00 ;
5.09E+01 ; -2.23E+02 ; -4.09E+00 ];
h24=[5.09E+01 ; -2.24E+02 ; 4.13E+00 ;
5.13E+01 ; -2.17E+02 ; 4.30E+00 ;
5.16E+01 ; -2.10E+02 ; 4.22E+00 ;
5.17E+01 ; -2.03E+02 ; 4.10E+00 ;
5.19E+01 ; -1.96E+02 ; 4.08E+00 ;
5.21E+01 ; -1.88E+02 ; 4.08E+00 ;
5.42E+01 ; -2.11E+02 ; 6.49E+00 ;
5.40E+01 ; -2.19E+02 ; 6.63E+00 ;
5.38E+01 ; -2.27E+02 ; 6.72E+00 ;
5.37E+01 ; -2.34E+02 ; 6.59E+00 ;
5.34E+01 ; -2.41E+02 ; 6.66E+00 ;
5.29E+01 ; -2.48E+02 ; 7.03E+00 ];
h25=[4.17E+01 ; -2.06E+02 ; -1.36E+00 ;
4.21E+01 ; -2.00E+02 ; -1.12E+00 ;
4.25E+01 ; -1.95E+02 ; -1.15E+00 ;
4.28E+01 ; -1.90E+02 ; -1.29E+00 ;
4.31E+01 ; -1.84E+02 ; -1.28E+00 ;
4.35E+01 ; -1.78E+02 ; -1.24E+00 ;
4.34E+01 ; -1.78E+02 ; 1.43E+00 ;
4.31E+01 ; -1.84E+02 ; 1.47E+00 ;
```

```
4.28E+01 ; -1.90E+02 ; 1.48E+00 ;
4.25E+01 ; -1.95E+02 ; 1.33E+00 ;
4.21E+01 ; -2.01E+02 ; 1.31E+00 ;
4.16E+01 ; -2.06E+02 ; 1.55E+00 ];
h26=[4.25E+01 ; -2.17E+02 ; -6.73E+00 ;
4.30E+01 ; -2.12E+02 ; -6.42E+00 ;
4.34E+01 ; -2.07E+02 ; -6.39E+00 ;
4.37E+01 ; -2.01E+02 ; -6.55E+00 ;
4.40E+01 ; -1.95E+02 ; -6.52E+00 ;
4.44E+01 ; -1.89E+02 ; -6.42E+00 ;
4.25E+01 ; -1.67E+02 ; -3.71E+00 ;
4.22E+01 ; -1.73E+02 ; -3.72E+00 ;
4.19E+01 ; -1.78E+02 ; -3.74E+00 ;
4.16E+01 ; -1.84E+02 ; -3.88E+00 ;
4.12E+01 ; -1.89E+02 ; -3.95E+00 ;
4.08E+01 ; -1.94E+02 ; -3.78E+00 ];
h27=[4.08E+01 ; -1.94E+02 ; 3.96E+00 ;
4.13E+01 ; -1.89E+02 ; 4.12E+00 ;
4.16E+01 ; -1.84E+02 ; 4.04E+00 ;
4.19E+01 ; -1.78E+02 ; 3.91E+00 ;
4.22E+01 ; -1.72E+02 ; 3.89E+00 ;
4.26E+01 ; -1.67E+02 ; 3.88E+00 ;
4.43E+01 ; -1.89E+02 ; 6.60E+00 ;
4.40E+01 ; -1.95E+02 ; 6.69E+00 ;
4.36E+01 ; -2.01E+02 ; 6.73E+00 ;
4.34E+01 ; -2.07E+02 ; 6.57E+00 ;
4.30E+01 ; -2.12E+02 ; 6.60E+00 ;
4.25E+01 ; -2.18E+02 ; 6.91E+00 ];
h28=[4.99E+01 ; -2.12E+02 ; 9.64E+00 ;
5.02E+01 ; -2.05E+02 ; 9.71E+00 ;
5.05E+01 ; -1.98E+02 ; 9.55E+00 ;
5.07E+01 ; -1.91E+02 ; 9.42E+00 ;
5.09E+01 ; -1.84E+02 ; 9.36E+00 ;
5.11E+01 ; -1.77E+02 ; 9.29E+00 ;
5.53E+01 ; -2.23E+02 ; 1.18E+01 ;
5.51E+01 ; -2.31E+02 ; 1.21E+01 ;
5.49E+01 ; -2.39E+02 ; 1.22E+01 ;
5.48E+01 ; -2.46E+02 ; 1.21E+01 ;
```

```
5.45E+01 ; -2.53E+02 ; 1.22E+01 ;
5.40E+01 ; -2.61E+02 ; 1.27E+01 ];
h29=[4.00E+01 ; -1.83E+02 ; 9.25E+00 ;
4.04E+01 ; -1.77E+02 ; 9.34E+00 ;
4.08E+01 ; -1.72E+02 ; 9.20E+00 ;
4.10E+01 ; -1.67E+02 ; 9.08E+00 ;
4.14E+01 ; -1.61E+02 ; 9.02E+00 ;
4.17E+01 ; -1.55E+02 ; 8.97E+00 ;
4.52E+01 ; -2.01E+02 ; 1.18E+01 ;
4.49E+01 ; -2.07E+02 ; 1.20E+01 ;
4.45E+01 ; -2.13E+02 ; 1.20E+01 ;
4.43E+01 ; -2.19E+02 ; 1.19E+01 ;
4.38E+01 ; -2.24E+02 ; 1.19E+01 ;
4.33E+01 ; -2.29E+02 ; 1.23E+01 ];
h30=[5.40E+01 ; -2.61E+02 ; -1.26E+01 ;
5.45E+01 ; -2.53E+02 ; -1.22E+01 ;
5.48E+01 ; -2.46E+02 ; -1.20E+01 ;
5.50E+01 ; -2.39E+02 ; -1.21E+01 ;
5.51E+01 ; -2.31E+02 ; -1.20E+01 ;
5.53E+01 ; -2.23E+02 ; -1.18E+01 ;
5.10E+01 ; -1.76E+02 ; -9.25E+00 ;
5.08E+01 ; -1.84E+02 ; -9.32E+00 ;
5.06E+01 ; -1.91E+02 ; -9.38E+00 ;
5.05E+01 ; -1.98E+02 ; -9.52E+00 ;
5.02E+01 ; -2.05E+02 ; -9.67E+00 ;
4.98E+01 ; -2.11E+02 ; -9.59E+00 ];
```

A.3 Permutation Matrix

```
%Pivoted QR Factorization
%[Q,R,P]=qr(VH,'vector');
[Q,R,P]=qr(VH);

%Permuted vectors
VP= V*P;
```